CHUA'S OSCILLATOR:
A ZOO OF ATTRACTORS

by

Philippe Deregel

Memorandum No. UCB/ERL M92/131

27 November 1992

CHUA'S OSCILLATOR:
A ZOO OF ATTRACTORS

by

Philippe Deregel

Memorandum No. UCB/ERL M92/131

27 November 1992

ELECTRONICS RESEARCH LABORATORY

College of Engineering
University of California, Berkeley
94720

CHUA'S OSCILLATOR:
A ZOO OF ATTRACTORS

by

Philippe Deregel

Memorandum No. UCB/ERL M92/131

27 November 1992

ELECTRONICS RESEARCH LABORATORY

College of Engineering
University of California, Berkeley
94720

CHUA'S OSCILLATOR : A ZOO OF ATTRACTORS

Philippe DEREGEL
Department of Aeronautics and Astronautics,
Stanford University,
Stanford, CA 94305-4035, USA

November 27, 1992

Abstract

Chaos has been widely reported and studied in Chua's circuit family, which is characterized by a 21 parameter family of odd-symmetric piecewise-linear vector fields in R^3. In this tutorial paper, we shall prove that, up to a topological equivalence, all the dynamics of this family are subsumed within that of a single circuit : *Chua's oscillator*; directly derived from Chua's circuit by adding a resistor in series with the inductor. We provide explicit formulas of the parameters of Chua's oscillator leading to a behavior qualitatively identical to that of any system belonging to Chua's circuit family. These formulas are then used to construct, in an almost trivial way, a gallery of (quasi-periodic and strange) attractors belonging to Chua's circuit family. A user-friendly program is available to allow a better understanding of the evolution of the dynamics as a function of the parameters of the canonical circuit, and to follow the trajectory in the eigenspaces.

1 Introduction

In this paper, we shall focus on a class of particularly simple three-dimensional chaotic systems : Chua's circuit family. This class of dynamical systems , henceforth denoted by $\mathcal{C}$, is characterized by a three-region, continuous, piecewise-linear vector field F with odd symmetry i.e. $F(-x) = -F(x)$ where we assume that there is no plane or line parallel to the boundary planes B_+ and B_- which is invariant under the action of F in the middle region (by continuity, this properties will also hold true for the outer regions). Since, as we shall see, the origin is an equilibrium point, this last assumption is equivallent to assuming that the eigenspaces [1] through the origin are not parallel to the boundary plane. As shown in Fig.1, the Jacobian matrices of the vector field F in the inner region D_0, and in the outer regions D_1 and D_{-1}, are denoted by M_0 and M_1, respectively. $\mathbf{b}$ is a vector of R^3, which ensures the continuity of F on the boundary planes B_+ and B_-. We shall denote by μ_1, μ_2 and μ_3 the eigenvalues of M_0, and by ν_1, ν_2 and ν_3 the eigenvalues of M_1. In order to avoid complex numbers, we shall introduce the following notation:

$$\left\{ \begin{array}{lllll} p_1 & = & \mu_1 + \mu_2 + \mu_3 & q_1 & = & \nu_1 + \nu_2 + \nu_3 \\ p_2 & = & \mu_1\mu_2 + \mu_2\mu_3 + \mu_3\mu_1 & q_2 & = & \nu_1\nu_2 + \nu_2\nu_3 + \nu_3\nu_1 \\ p_3 & = & \mu_1\mu_2\mu_3 & q_3 & = & \nu_1\nu_2\nu_3 \end{array} \right. \quad (1)$$

The fact that the elements of $\mathcal{C}$ can be considered as three affine systems glued together, each of which having a well-known solution, simplifies the theoretical study of these systems. These properties allow an in-depth study of the dynamics in $\mathcal{C}$. In particular, it has made it possible to give á rigorous proof of chaos in Chua's circuit [1]; an element of $\mathcal{C}$ [2] [3] shown in Fig.2(a) and known as the simplest autonomous circuit which exhibits chaos.

From a physical point of view, the circuits which belong to $\mathcal{C}$ are very simply built. They only have one nonlinear element : a Chua's diode [4], a five-region piecewise linear resistor whose i-v characteristic, in the

[1] eigenvector or eigenplane

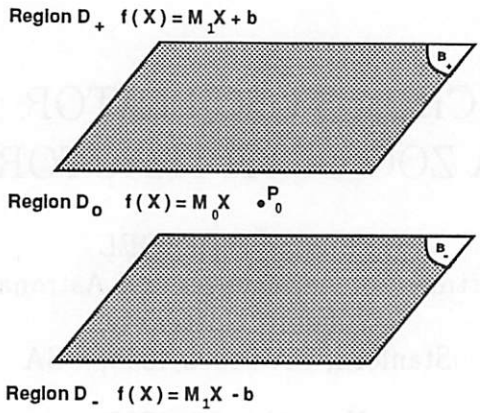

Figure 1: A three-region piecewise-linear system

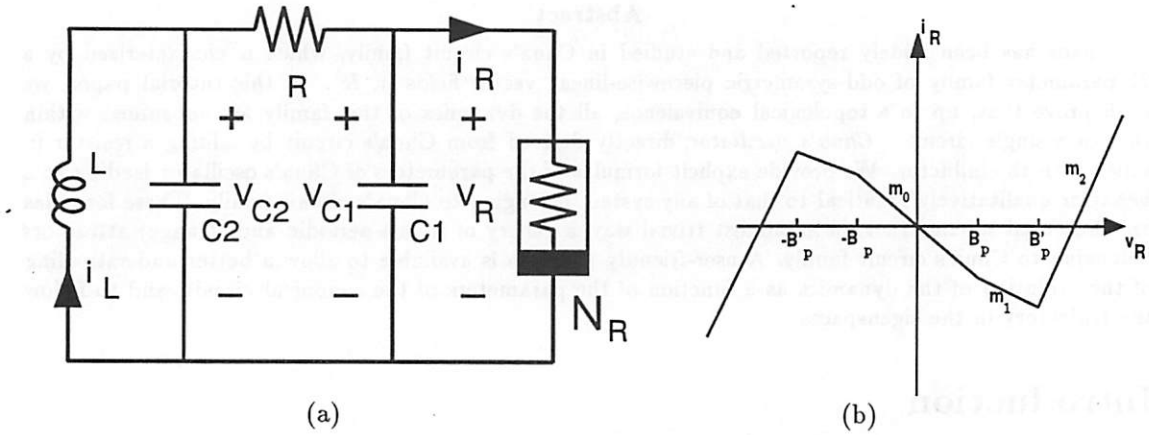

(a) (b)

Figure 2: (a) Chua's circuit (b) characteristic of Chua's diode

special case of Chua's circuit [2], is given in Fig.2(b). For other members of Chua's circuit family $\mathcal{C}$, the slopes m_0 and m_1 for the two inner segments may assume *any* real number, positive or negative. However, from a physical point of view, in a real circuit, the slope m_2 of the two outer segments is always positive, because otherwise the system could gain an infinite amount of energy which is physically impossible. However in most examples to date, these two segments do not play any interesting role in the chaotic dynamics. When a three-region system is simulated (without these outer segments), the trajectory might diverge, due to an improper choice of parameters or initial conditions. In this paper, we shall only include the two inner segments of slopes $m_0 < 0$ and $m_1 > 0$ as shown in Fig.3.

The possibility of a simple and robust realization of the elements of $\mathcal{C}$ is certainly an advantage for their study. This is all the more interesting since, as we shall see in this paper, there exists some circuits [5] which are imbued with all the complicated dynamics of $\mathcal{C}$. These circuits allow us to realize any eigenvalue patterns. The first circuit having these properties, namely: Chua's canonical circuit [6] [7] has been proposed in 1987. In this paper, we introduce another circuit having these properties: Chua's oscillator [8]. It is remarkable that this circuit is directly derived from Chua's circuit by adding only a linear a resistor in series with the inductor [2]. We shall first transform the state equations of Chua's oscillator into a dimensionless form. Then we shall give values of the parameters of Chua's oscillator, as well as those of its dimensionless form (after

[2]Note that in a real circuit it is impossible to realize a pure inductance, therefore it is logical to add a resistance in series with the inductance anyway.

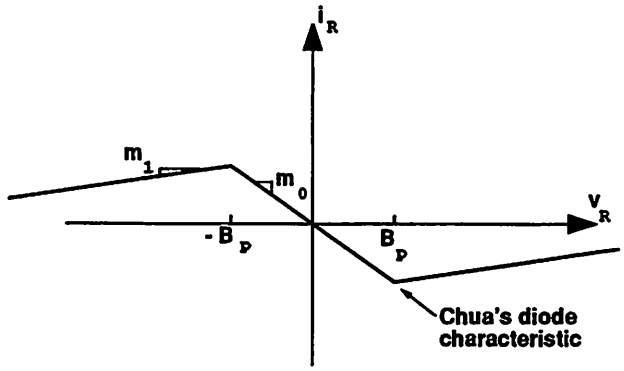

Figure 3: Three-region characteristic of Chua's diode

a time rescaling), correponding to any prescribed eigenvalue pattern [3]

$$(\mu;\nu) = (\mu_1, \mu_2, \mu_3; \nu_1, \nu_2, \nu_3) \quad \text{or} \quad (p;q) = (p_1, p_2, p_3; q_1, q_2, q_3) \tag{2}$$

If, as proven in section 5, two elements of $\mathcal{C}$ having the same eigenvalues exhibit the same qualitative behavior, all the complicated dynamics of $\mathcal{C}$ are subsumed within that of Chua's oscillator or its associated dimensionless form.

In section 3 we shall illustrate the properties of Chua's oscillator with some examples. We shall determine the parameters of Chua's oscillator and of its associated dimensionless form leading to some well-known attractors belonging to $\mathcal{C}$.

In section 4, we shall systematically determine them for all the attractors found so far in $\mathcal{C}$. For each attractor, we shall give the Lyapunov dimension, the eigenvalue pattern, the parameters of Chua's oscillator dimensionless form, and a phase portrait.

In section 5 we shall present some basic concepts relative to the dynamics of $\mathcal{C}$. In this tutorial paper, written for the non-specialist, this section can be considered as both a short introduction to chaotic dynamics and a simple answer to questions that might arise in the reading of the first four sections. In the same spirit, we wait for the end of this paper to prove that two elements of $\mathcal{C}$ having the same eigenvalues (μ, ν) exhibit the same dynamics. This is the basis of this paper and will be assumed in the first five sections.

2 Chua's oscillator

2.1 The circuit and its equations

Our aim in this section is to provide a circuit to realize any prescribed eigenvalue pattern associated with a vector field belonging to $\mathcal{C}$. First of all, since the system is of the third order, the circuit must have three-dynamic elements. In addition, since our objective is a three-region symmetric piecewise-linear continuous vector field, we can allow only one nonlinear resistor, the *Chua's diode* [4], whose v-i characteristic shown in Fig.3 is odd-symmetric and 3-segment piecewise linear. All other elements must be linear.

In an autonomous linear RC circuit which has two elements, there is only one natural frequency $\nu = 1$ / RC. Therefore, to produce a prescribed natural frequency, R or C can be assigned an arbitrary value (e.g., let C=1) and then the value of the other parameters can be calculated. In other words, to synthesize a circuit having n *arbitrarily prescribed* eigenvalues, at least $(n+1)$ circuit parameters are necessary.

If we are given 6 eigenvalues, then we need at least 7 parameters. We already have 3 dynamic elements and 2 slopes for the nonlinear resistor; therefore, 2 more linear resistors are the minimum requirement. The chosen circuit, so-called Chua's oscillator [5] [9] is shown in Fig.4. It is remarkable that this circuit is simply

[3]Note that $(\mu;\nu)$ is obtained from $(p;q)$ with (1). Conversely, μ_i (resp. ν_i) are the roots of the polynomial : $\mu^3 - p_1\mu^2 + p_2\mu - p_3 = 0$ (resp. $\nu^3 - q_1\nu^2 + q_2\nu - q_3 = 0$) . We shall assume without any loss of generality that μ_1 (resp. ν_1) is real.

obtained from Chua's circuit by adding a resistance R in series with the inductance. The state equations of Chua's oscillator, henceforth denoted by Σ_c are :

$$\Sigma_c \quad : \quad \begin{cases} C_1 \frac{dv_1}{dt} &= G(v_2 - v_1) - \hat{f}(v_1) \\ C_2 \frac{dv_2}{dt} &= G(v_1 - v_2) + i_3 \\ L \frac{di_3}{dt} &= -v_2 - Ri_3 \end{cases} \tag{3}$$

where

$$\hat{f}(v) = G_b v + \frac{1}{2}(G_a - G_b)(\mid v + B_p \mid - \mid v - B_p \mid) \tag{4}$$

is the v-i characteristic of the Chua's diode shown in Fig.3.

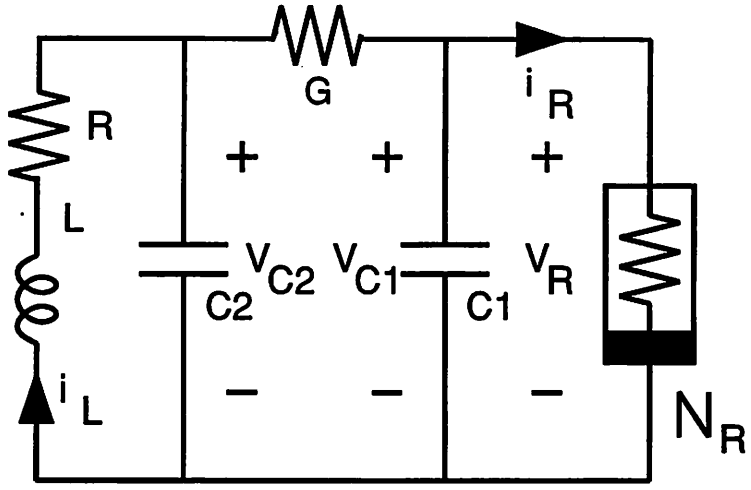

Figure 4: Chua's oscillator

We can transform the state equation Σ_c into a dimensionless form by defining :

$$\begin{array}{lll} x \equiv v_1/B_p & y \equiv v_2/B_p & z \equiv i_3/(B_p G) \\ \tau \equiv tG/C_2 & m_0 \equiv G_a/G & m_1 \equiv G_b/G \\ \alpha \equiv C_2/C_1 & \beta \equiv C_2/(LG^2) & \gamma \equiv C_2 R/(LG) \end{array} \tag{5}$$

The corresponding dimensionless state equations are given by :

$$\begin{cases} \dot{x} &= \alpha(y - x - f(x)) \\ \dot{y} &= x - y + z \\ \dot{z} &= -\beta y - \gamma z \end{cases} \tag{6}$$

where :

$$f(x) = m_1 x + \frac{1}{2}(m_0 - m_1)(\mid x + 1 \mid - \mid x - 1 \mid) \tag{7}$$

Note that in (6), $\dot{x} = \frac{dx}{d\tau}$ and also that thoughout the paper we shall assume that $B_p = 1$ which does not affect the dynamics [4] . The system (6) has a *qualitatively* identical behavior to that obtained from (3), provided that $G/C_2 > 0$. If $G/C_2 < 0$, an attractor in (3) becomes a "repeller" in (6) because the dimensionless time $\tau < 0$ when $t > 0$. Hence, we have a negative *time rescaling* in (5). In this case, we can still use (6) to obtain an attractor of (3) , by merely integrating (6) *backwards* in time. This is equivalent to integrating the following alternate dimensionless equation in forward time:

$$\begin{cases} \dot{x} &= \alpha(x - y + f(x)) \\ \dot{y} &= y - x - z \\ \dot{z} &= \beta y + \gamma z \end{cases} \tag{8}$$

[4] If $B_p \neq 1$, we simply divide x, y and z by B_p to find the solution of Σ_c

where the parameters α, β and γ and the function f are the same as in (6). Equations (6) and (8) can be combined into a single equation :

$$\Sigma_{\mathrm{d}} \quad : \qquad \begin{cases} \dot{x} &= k\alpha(y - x - f(x)) \\ \dot{y} &= k(x - y + z) \\ \dot{z} &= k(-\beta y - \gamma z) \end{cases} \tag{9}$$

where $k = 1$ if $G/C_2 > 0$ and $k = -1$ if $G/C_2 < 0$. Equations (9), henceforth denoted by Σ_d are known as the *Chua's oscillator dimensionless equations.* Observe that we only have five dimensionless parameters $\alpha, \beta, \gamma, m_0$ and m_1, compared to the twenty one parameters required to completely define an element of $\mathcal{C}$, as shown in Fig.1.

Let us first assume, as it will be proven in section 5, that the qualitative behavior of $\mathcal{C}$ is determined by its six eigenvalues : $\mu_1, \mu_2, \mu_3, \nu_1, \nu_2$ and ν_3. As we shall see, in the outer regions, for all the examples presented in this paper, we shall always find one real and two complex conjugate eigenvalues that can be denoted by :

$$\nu_1 = \gamma_1 \quad \nu_2 = \sigma_1 + j\omega_1 \quad \nu_3 = \sigma_1 - j\omega_1 \tag{10}$$

Since we are only interested in preserving the qualitative behavior of the system, we can assume that $\omega_1 = 1$ so that only five parameters need to be matched by those of Σ_d. This assumption is equivalent to a change in the time scale and hence involves no loss of generality. Note that if the eigenvalues in the outer regions were all real, we could assume one eigenvalue, for example ν_1, to have a norm equal to 1 and proceed as above.

2.2 Explicit formulas for calculating the parameters of Chua's oscillator

Given any prescribed set of eigenvalues, [5] gives the explicit formulas for calculating the circuit parameters C_1, C_2, L, R, G, G_a and G_b of the Chua's oscillator shown in Fig. 4. As mentioned before, among the seven parameters, we can assign an arbitrary value to any one of them. Assuming $C_1 = 1$, the other circuit parameters are given as follows :

$$\begin{cases} C_2 = \frac{1}{k_1 k_2^2} \\ G = \frac{1}{k_2} \\ G_a = -p_1 - \frac{1}{k_2} - \frac{p_2 - q_2}{p_1 - q_1} \\ G_b = -q_1 - \frac{1}{k_2} - \frac{p_2 - q_2}{p_1 - q_1} \\ L = \frac{1}{k_1 k_2^2 k_3} \\ R = -1 + \frac{1}{k_1^2 k_2^4 k_3} \frac{p_3 - q_3}{p_1 - q_1} \end{cases} \tag{11}$$

where:

$$\begin{cases} k_1 = -p_3 + \frac{q_3 - p_3}{q_1 - p_1} \left(p_1 + \frac{p_2 - q_2}{q_1 - p_1} \right) \\ k_2 = p_2 - \frac{q_3 - p_3}{q_1 - p_1} + \frac{p_2 - q_2}{q_1 - p_1} \left(\frac{p_2 - q_2}{q_1 - p_1} + p_1 \right) \\ k_3 = \frac{p_2 - q_2}{q_1 - p_1} - \frac{k_1}{k_2} \end{cases} \tag{12}$$

Observe that the parameters *cannot* be found whenever the denominator in one of the equations (11) or (12) is equal to zero. This is the case when :

$$p_1 = q_1 \tag{13}$$

or

$$-p_3 + \frac{q_3 - p_3}{q_1 - p_1} \left(p_1 + \frac{p_2 - q_2}{q_1 - p_1} \right) = 0 \tag{14}$$

or

$$p_2 - \frac{q_3 - p_3}{q_1 - p_1} + \frac{p_2 - q_2}{q_1 - p_1} = 0 \tag{15}$$

or

$$\frac{p_2-q_2}{q_1-p_1}-\frac{-p_3+\frac{q_3-p_3}{q_1-p_1}\left(p_1+\frac{p_2-q_2}{q_1-p_1}\right)}{p_2-\frac{q_3-p_3}{q_1-p_1}+\frac{p_2-q_2}{q_1-p_1}}=0 \tag{16}$$

Each of these four equations (13)-(16) represents a 5-dimensional hyper-surface in the six-dimensional space $(p_1,...q_3)$. The eigenvalue patterns that cannot be realized *exactly* by Chua's oscillator belong to one of these four hyper-surfaces, and therefore constitute a set of measure zero; we shall denote it by S_c. Given an eigenvalue pattern $(p;q)$, we can always perturb it in order to obtain :

$$(p_1+\delta p_1, p_2+\delta p_2, p_3+\delta p_3; q_1+\delta q_1, q_2+\delta q_2, q_3+\delta q_3) \tag{17}$$

where δp_i and δq_i are arbitrarily small, so that the resulting eigenvalue pattern (16) does not belong to S_c and hence can be generated by Chua's oscillator. If δp_i and δq_i are chosen sufficiently small, which is always possible since S_c is a zero-measure set, it follows that by the continuity property of ODE with respect to parameters, that the qualitative behavior of the system will be preserved. We will illustrate this with examples in section 3.

2.3 Explicit formulas for calculating the parameters of Chua's oscillator dimensionless equations

Our aim is now to obtain the parameters of Chua's oscillator dimensionless equations as a function of the eigenvalues. Consider an eigenvalue pattern (μ,ν) and its corresponding circuit parameters obtained from (11). From these circuit parameters we can determine the dimensionless parameters from (5), assuming in the process of finding the parameters *and* the time rescaling, we do not encounter any denominator having a value equal to zero. Regarding the time rescaling $\tau=tG/C_2$, it follows from (11) that it cannot be equal to zero. The fact that the time rescaling cannot be found equal to zero is an interesting property of Chua's oscillator that Chua's canonical circuit does not have (see [7]). We shall denote by S_d the zero-measure set of eigenvalues for which we cannot find the dimensionless parameters; note that $S_d \subset S_c$. Also note that (except for $|G/C_2|=1$, which is a zero-measure set), when we find the dimensionless parameters coresponding to (μ,ν), this does not mean that the eigenvalues of Σ_d are $(\mu;\nu)$, *but* that there exists a system Σ_c, that has the eigenvalues (μ,ν) and whose dynamics is equivalent to that of Σ_d (up to a positive time rescaling). Therefore Σ_d has the same qualitative behavior as any element of $\mathcal{C}$ having the eigenvalues (μ,ν).

In order to obtain directly the parameters of Chua's oscillator dimensionless equations as a function of the eigenvalues, we can substitute (11) into (5). Another possibility consists of directly deriving these formulas from (9). Fortunately, in both cases, i.e., by substitution of (11) into (5) or by direct derivation, we find the same result :

$$\begin{cases} \alpha=\frac{1}{K_1K_2^2} \\ \beta=K_3K_2^2 \\ \gamma=-K_2^2K_3+\frac{1}{k1^2k_2^2}\frac{p_3-q_3}{q_1-p_1} \\ m_0=-1-\left(p_1+\frac{p_2-q_2}{q_1-p_1}\right)K_2 \\ m_1=-1-\left(q_1+\frac{p_2-q_2}{q_1-p_1}\right)K_2 \\ k=sgn(K_1K_2) \end{cases} \tag{18}$$

where:

$$\begin{cases} k_1=-p_3+\frac{q_3-p_3}{q_1-p_1}\left(p_1+\frac{p_2-q_2}{q_1-p_1}\right) \\ k_2=p_2-\frac{q_3-p_3}{q_1-p_1}+\frac{p_2-q_2}{q_1-p_1}\left(\frac{p_2-q_2}{q_1-p_1}+p_1\right) \\ k_3=\frac{p_2-q_2}{q_1-p_1}-\frac{k_1}{k_2} \end{cases} \tag{19}$$

The zero-measure set for which the parameters of Chua's oscillator dimensionless equations *cannot* be determined is defined by any one of the following constraints :

$$p_1=q_1 \tag{20}$$

or

$$-p_3+\frac{q_3-p_3}{q_1-p_1}\left(p_1+\frac{p_2-q_2}{q_1-p_1}\right)=0 \tag{21}$$

or

$$p_2-\frac{q_3-p_3}{q_1-p_1}+\frac{p_2-q_2}{q_1-p_1}\left(\frac{p_2-q_2}{q_1-p_1}+p_1\right)=0 \tag{22}$$

Note first that (20), (21) and (22) are the same as (13), (14) and (15) respectively. Second, in (5), only $1/L$ appears (not L), and assuming that $p_1 \neq q_1$,$1/L$ always exists (see (11)); that is why (16) is not present in S_d.

2.4 Equilibrium points and eigenspaces

In this section we shall determine the equilibrium points and the eigenspaces corresponding to the Chua's oscillator dimensionless equations. These formulas constitute the basis of a user-friendly program, presented in Appendix A, that determines the equilibrium points and displays the trajectory in the eigenspaces, starting from any initial conditions. Let us first determine the equilibrium points [5] of Chua's canonical equations. Consider the equilibria:

$$\begin{cases} y-x-f(x) &= 0 \\ x-y+z &= 0 \\ \beta y+\gamma z &= 0 \end{cases} \tag{23}$$

From a physical point of view, (23) can be interpreted as the equations of the circuit at dc, when the capacitors are open-circuited and the inductor short-circuited. The equation of the load line is:

$$w=-\frac{\beta}{\gamma+\beta}x \quad \text{where } w = \text{y-x} \tag{24}$$

The only interesting case, which can lead to complicated dynamics, is when the circuit has three dc-operating points. The nonlinear function $F(\cdot)$ and the load line are shown in Fig.5.

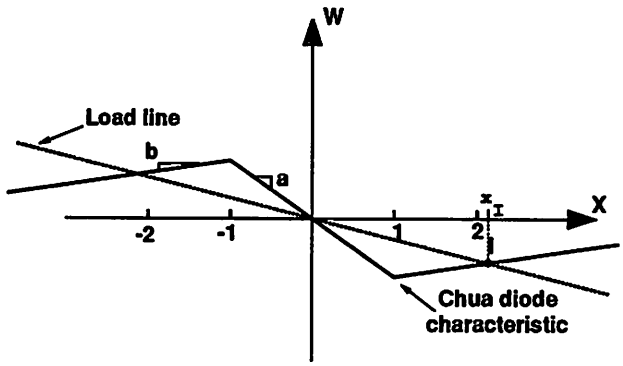

Figure 5: dc operating points of the Chua diode

The load line intersects the outer segment if and only if the operating point I has an abscissa :

$$x_I=\frac{\mathrm{m_0}-\mathrm{m_1}}{\mathrm{m_1}+\frac{\beta}{\gamma+\beta}} \tag{25}$$

greater than 1 as in Fig.5, leading to an equilibrium point in each of the three regions.

$$\begin{cases} P_+ &= (x_I, \frac{\gamma}{\gamma+\beta}x_I, -\frac{\beta}{\gamma+\beta}x_I) & \in D_+ \\ P_0 &= (0,0,0) & \in D_0 \\ P_- &= (-x_I, -\frac{\gamma}{\gamma+\beta}x_I, \frac{\beta}{\gamma+\beta}x_I) & \in D_- \end{cases}$$

[5] In our case, the equilibrium points are the points where the vector field is equal to zero

In the case of three equilibrium points, let us now study their stability, i.e., the nature of the eigen spaces present in the neighborhood of P_+,$P_0$and P_-. One of the advantages of a piecewise-linear vector field is that in each region these eigenvalues are constants and the eigen spaces (plane or eigenvector) are constant, therefore we do not have to do any local approximation in order to determine the Jacobian matrices of the system. Let us first examine the stability of the origin P_0. In the region D_0 the state equation is :

$$\dot{X} = M_0 X \tag{26}$$

where the Jacobian matrix is the constant matrix :

$$M_0 = k \begin{pmatrix} -1-m_0 & 1 & 0 \\ 1 & -1 & 1 \\ 0 & \beta & \gamma \end{pmatrix} \tag{27}$$

and its chracteristic polynomial is :

$$\begin{aligned} |\,\lambda I - M_0\,| \;=\; & \lambda^3 + k\lambda^2(2+m_0-\gamma) \\ & +\lambda((1-\gamma)(1+m_0)-\gamma+\beta-1) \\ & +k(-(m_0+1)(\gamma+\beta)+\gamma) = 0 \end{aligned} \tag{28}$$

The eigenvalues of the Chua's canonical equations are the roots of (28). In order to determine the type of the eigenvalue pattern associated with M_0, let us introduce Γ :

$$\begin{aligned} \Gamma \;=\; & \tfrac{1}{9}\left[3((1-\gamma)(1+m_0)-\gamma+\beta-1)-(2+m_0-\gamma)^2\right]^2 \\ & +\tfrac{1}{3^{12}}[2k(2+m_0-\gamma)^3 - 9k(2+m_0-\gamma)(\gamma(2+m_0-\gamma) \\ & +27k(-(m_0+1)(\gamma+\beta)+\gamma)]^3 \end{aligned} \tag{29}$$

According to the value of Γ, there are three different cases:
(a) ($\Gamma > 0$) : one real and two complex conjugate eigenvalues
(b) ($\Gamma = 0$) : three real eigenvalues of which at least two are equal.
(c) ($\Gamma < 0$) : three real and unequal eigenvalues.

If we have determined the dimensionless parameters from an eigenvalue pattern $(\mu;\nu)$, we already know the type of eigenvalue pattern. However as we have already noticed, the eigenvalues of Σ_d are not $(\mu;\nu)$ but $|k_1 k_2|(\mu;\nu)$ where k_1 and K_2 are given in (18). This multiplication of the eigenvalues by a *positive* coefficient does not affect the qualitative behavior of the system. After having found the eigenvalues of Σ_d, in each of the three cases (a),(b) and (c), we shall determine the corresponding eigen spaces:

Case(a) The eigenvector V_{λ_R}, corresponding to the real eigenvalue λ_R, is determined up to a multiplicative constant by:

$$M_0 V_{\lambda_R} = \lambda_R V_{\lambda_R} \tag{30}$$

and a solution of (26) is:

$$V_\lambda = \begin{pmatrix} 1 \\ m_0+1+\lambda_R \\ \frac{m_0+\lambda_R+1}{\lambda_R-\gamma} \end{pmatrix} \tag{31}$$

Note that if λ were equal to γ, (30) would imply that β is equal to zero. This would mean that the last equation of (9) is uncoupled which cannot lead to any interesting behavior. The eigenplane P_0 corresponding to the complex conjugate eigenvalues

$$\lambda_{C\pm} = u \pm iv \tag{32}$$

is determined as a linear combination of the two vectors U and V such that:

$$\begin{pmatrix} A-uI & vI \\ A-vI & -uI \end{pmatrix} \begin{pmatrix} U \\ V \end{pmatrix} = 0 \tag{33}$$

By definition of u and v, the determinant of the linear system (33) which has six unknowns and 6 equations is equal to zero. By giving an arbitrary value to one of the coordinates of U or V, we obtain a full rank,

namely, 5, Cramer system that can be easily solved by classical methods. Note that $\Gamma \neq 0$ implies that there exists such a fifth-order Cramer system of equations in (33).

Case(b) This case corresponds to a measure-zero set of parameters. Therefore, as it has been explained in 2.2, it is possible to slightly perturb the parameters without changing the behavior of the system and obtain a system that belongs to case (a), or in the following case (c). This case could also have been directly treated.

Case(c) The coordinates of the three eigenvectors corresponding to the real eigenvalues λ_R can directly be determined by (31).

The study of the stability of the outer equilibrium points is very similar to that at P_0, except that the Jacobian matrix of the vector field is now:

$$M_1 = k \begin{pmatrix} -1-m_1 & 1 & 0 \\ 1 & -1 & 1 \\ 0 & \beta & \gamma \end{pmatrix} \tag{34}$$

Therefore, we can determine the eigenvalues and eigenspaces in the outer regions by substituing m_1 into m_0 in the equations obtained in the inner region. In the next section, we shall examine examples of eigenvalue and eigenspace patterns in $\mathcal{C}$

3 Mapping other chaotic circuits and systems into Chua's oscillator

3.1 Introduction

In this section, we have two objectives. First we want to show with some well-known examples that it is easy to obtain the dynamics of any elements[6] of $\mathcal{C}$ from Chua's oscillator and from its associated dimensionless system. In each case we shall verify that we find the same trajectory with Chua's oscillator dimensionless equations as with the original system [7] (the trajectories are copied from the original paper). Second, we shall take advantage of these examples to present some aspects of the dynamics in $\mathcal{C}$, in particular the role of the eigenspace and the eigenvalues in the dynamics of an element of $\mathcal{C}$.

For each element of $\mathcal{C}$ considered in this section, we shall give the expression of the vector field before giving the eigenvalue pattern corresponding to each attractor. To avoid any confusion with the notations, the parameters relative to the original system will have a tilde (i.e. $\tilde{\alpha}, \tilde{\beta}$....) . All these systems belong to $\mathcal{C}$, therefore they have the same three-region piecewise linear nonlinearity:

$$\tilde{f}(x) = \tilde{m}_1 x + \frac{1}{2}(\tilde{m}_0 - \tilde{m}_1)(|x+1| - |x-1|) \tag{35}$$

When there are three real eigenvalues in the middle region D_0, (μ, ν) is said to be of *type I*. If there is one real and two complex conjugate eigenvalues in D_0, (μ, ν) is said to be of *type II*.

3.2 Three examples of attractors from Chua's circuit

The dimensionless form of Chua's circuit state equations [10] [11] [12] is :

$$\begin{cases} \dot{x} &= \tilde{\alpha}\left(y - x - \tilde{f}(x)\right) \\ \dot{y} &= x - y + z \\ \dot{z} &= -\tilde{\beta} y \end{cases} \tag{36}$$

As shown earlier in this paper, Chua's oscillator is directly derived from Chua's circuit, therefore it is easy to obtain the parameters of Σ_c or of Σ_d or of its associated dimensionless form by merely keeping the same values of circuit parameters and dimensionless coefficients *and* choosing $R = 0$ and $(\gamma = 0, k = 1)$[8] ,

[6] Chua's circuit, Chua's torus circuit, Ogorzalec ladder circuit, Brockett and Sparrow's systems

[7] with the restrictions introduced in section 5

[8] $\alpha = \tilde{\alpha}, \beta = \tilde{\beta}, m_0 = \tilde{m}_0, m_1 = \tilde{m}_1$

respectively. Since the vector field corresponding to Σ_d is exactely the same as the original dimensionless form of Chua's circuit, the trajectories will be the same. We do not have to verify that the trajectories are identical, but we shall take advantage of the next three examples to introduce some basic concepts relative to piecewise linear sytems.

3.2.1 Rössler-type attractor.

For $\tilde{\alpha} = 8.5, \tilde{\beta} = 14.28, \tilde{m}_0 = -8/7$, and $\tilde{m}_1 = 5/7$, (36) has a chaotic attractor [13], as shown in Fig.6-a,. This corresponds to the following set of eigenvalues :

$$\begin{cases} \mu_1 = 0.677 & \mu_2 = -0.304 + j0.901 & \mu 3 = -0.304 - j0.901 \\ \nu_1 = -1.22 & \nu_2 = -0.304 + j1.00 & \nu_3 = -0.304 - j1.00 \end{cases} \tag{37}$$

The trajectory obtained from the dimensionless equations of Chua's oscillator is shown in Fig.6-a. Suppose that starting from the initial conditions (x_0, y_0, z_0) we obtain the trajectory T_1 shown in Fig. 6-a. If we change the initial conditions into $(-x_0, -y_0, -z_0)$, we would obtain a trajectory which is the symmetric image of T_1 with respect to the origin, as shown in Fig.6-b. Provided that the vector field Σ_d is symmetric with respect to the origin, if we find a trajectory T from any element of $\mathcal{C}$, it is *always* possible to find its symmetric "twin" by choosing the associated odd-symmetric initial conditions. Note that the symmetric image of T is T itself for all odd-symmetric *periodic* orbit. Our attractor in the next example appears also to be odd symmetric, however it is only an illusion, since the double scroll presented below *cannot* be periodic. Indeed with sufficient computer precision, one can always find its distinct symmetric twin, which will look almost identical to its twin.[9]

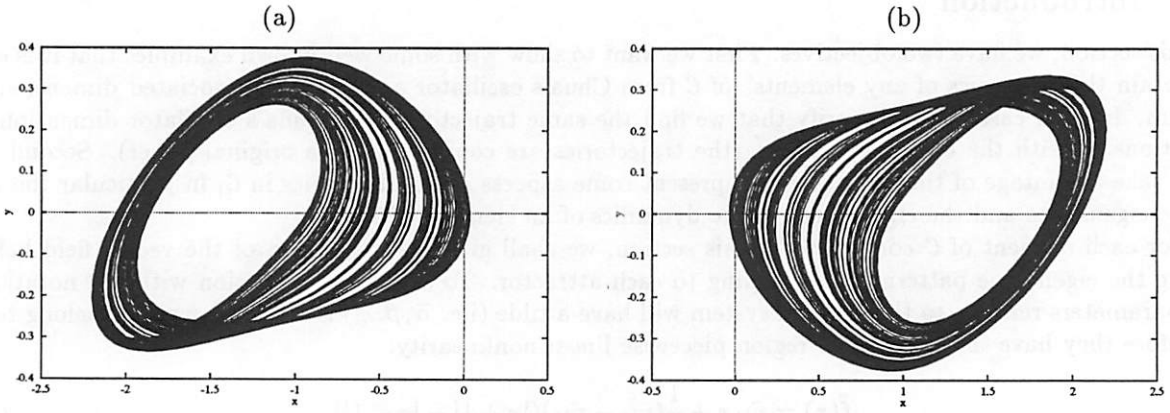

Figure 6: A Rössler-type attractor and its odd-symmetric twin obtained from Σ_d

3.2.2 The Double Scroll attractor

For $\tilde{\alpha} = 9, \tilde{\beta} = 14.28, \tilde{m}_0 = -1/7$ and $\tilde{m}_1 = 2/7$, (36) has a chaotic attractor [14] [15], called the *double scroll*, as shown in Fig. 7. This corresponds to the following set of eigenvalues :

$$\begin{cases} \mu_1 = 0.728 & \mu_2 = -0.317 + j0.889 & \mu_3 = -0.317 - j0.889 \\ \nu_1 = -1.29 & \nu_2 = 0.0608 + j1.00 & \nu_3 = 0.0608 - j1.00 \end{cases} \tag{38}$$

Observe that the double scroll attractor can be considered as the result of the merging of the two Rössler attractors shown in Figs.6-a - 6-b.

A typical trajectory of the double scroll and its eigenspaces are shown in Fig.8. The eigenvalue pattern (μ, ν) is of type II; in each region, there is one eigenvector corresponding to the real eigenvalue and one eigenplane corresponding to the two complex conjugate eigenvalues. One can recognize in Fig.8 a middle

[9] see section 5 for more details

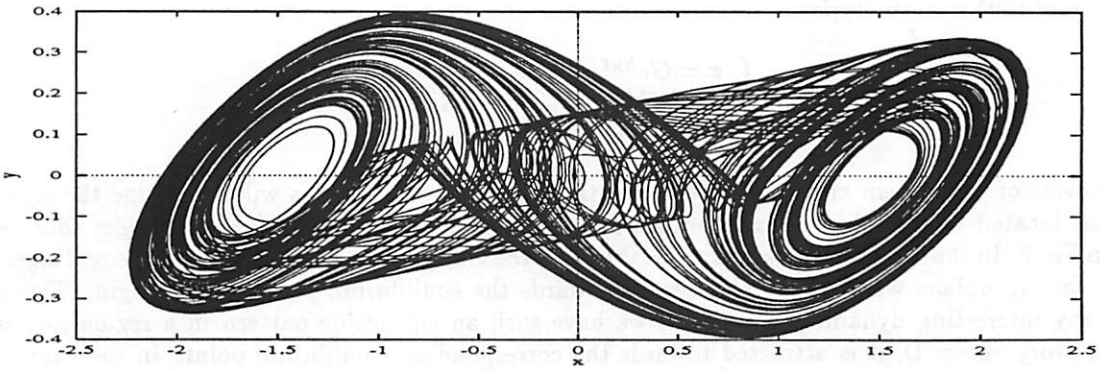

Figure 7: Phase portrait of the double scroll attractor obtained from Σ_d

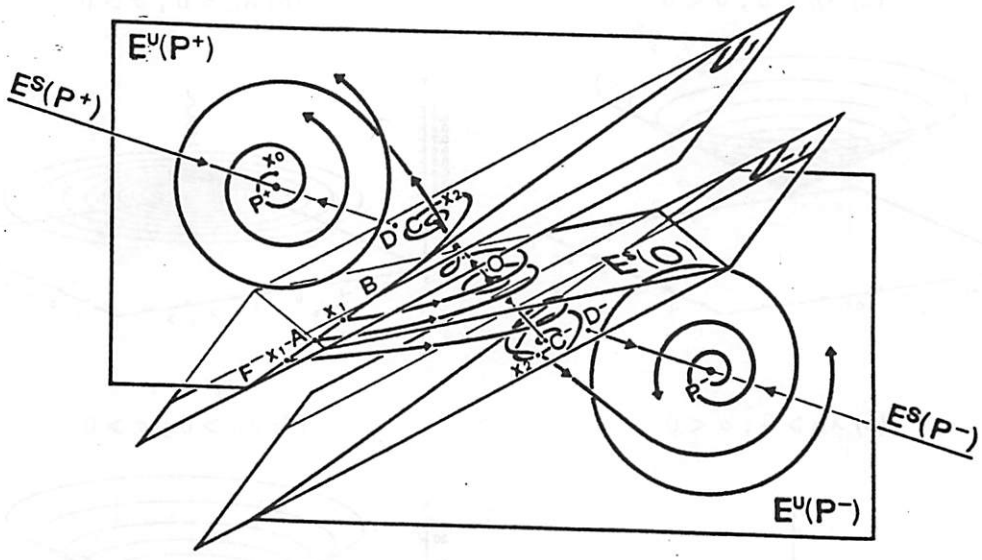

Figure 8: Typical trajectories and eigen spaces for the double scroll attractor

region D_0, separated by the two boundary planes U_1 and U_{-1}, an upper outer region D_1 which is the half space above U_1, and a lower outer regions D_{-1} which is the symmetric image of D_1 with respect to the origin O. As pointed out earlier, one of the advantages of $\mathcal{C}$ is that in each region (D_{-1},D_0 and D_1), the system is affine, therefore it has a well-known behavior. Before going any further, let us recall the solution of a linear [10] system whose dynamics are determined by a state equation of the type:

$$\dot{X} = MX \tag{39}$$

If the matrix has one real eigenvalue λ_R and two complex-conjugate eigenvalues $\lambda_{C\pm} = \sigma \pm j\omega$, there exists a basis B where the matrix M is in the form [11] :

$$\begin{pmatrix} \lambda_R & 0 & 0 \\ 0 & \sigma & -\omega \\ 0 & \omega & \sigma \end{pmatrix} \tag{40}$$

[10] We assume that the origin of the basis B is located at an equilibrium point

[11] Namely, the real Jordon form

A solution of (39) is of the type :

$$\begin{cases} x = Ge^{\lambda_R t} \\ y = e^{\sigma t}(Hcos(\omega t) - Ksin(\omega t)) \\ z = e^{\sigma t}(Hsin(\omega t) + Kcos(\omega t)) \end{cases} \tag{41}$$

The behavior of the system crucially depends on the sign of λ_R and σ, this will determine the sign of the coefficient located before t in the exponentials in the equations (41) . We have to consider four cases as shown in Fig.9. In the case (a), the system is stable, and the trajectory is attracted along the real eigenvector towards the eigenplane where it spirals inwards towards the equilibrium point at the origin. This cannot lead to any interesting dynamics, because if we have such an eigenvalue pattern in a region D_i, as soon as a trajectory enters D, it is attracted towards the corresponding equilibrium point. In the case (b), the trajectory is attracted towards the eigenplane while spiraling outwards. In the case (c), the trajectory spirals inwards while diverging along the real eigenvactor. In the last case (d), the trajectory spirals outwards while diverging along the real eigenvector.

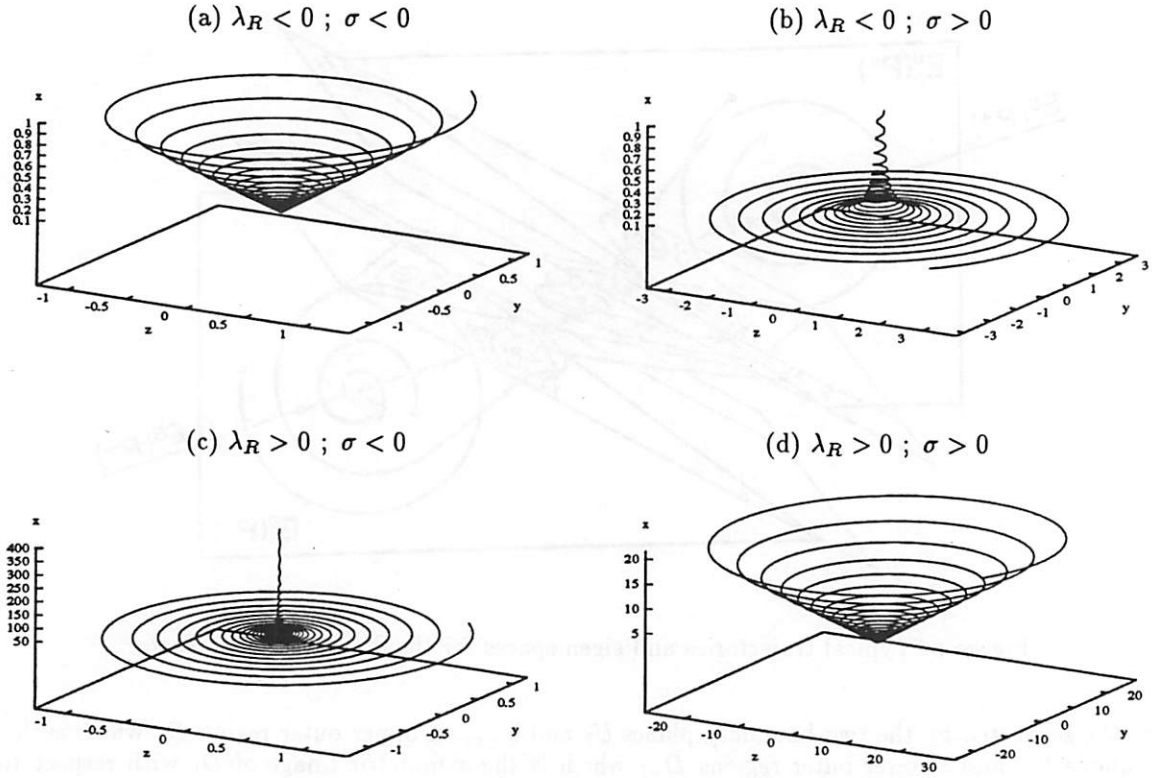

Figure 9: Four types of trajectory in an affine system with one real and two complex-conjugate eigenvalues

For the double scroll, we have case(c) in the middle region and case (b) in the outer regions. Let us for example start from a point X_0 in the region D_1. The trajectory is strongly ($\nu_1 \ll 0$) attracted towards the eigenplane $E^U(P^+)$ while it spirals outwards. Since we have assumed that in $\mathcal{C}$ no eigenspace can be parallel to the boundary plane, it follows that the trajectory must exit from D_1. In D_0, we have case (b), the trajectory spirals inwards in $E^S(0)$, and diverges along the real eigenvector $E^S(O)$. Schematically, as shown in Fig.8, if a trajectory enters D_0 above $E^S(0)$ it will return to D_1, and if it enters D_0 below $E^S(0)$ it will go to D_{-1}. Thus, one can easily understand the evolution of the trajectory. However, although deterministic, it cannot be predicted exactly over a long period of time as it is chaotic. For us, this means that the system exhibits a sensitive dependence on the initial conditions. If instead of starting from x_0, we started from a point

x_0' infinitesimally close to x_0 (but different), we would eventually find two different uncorrelated trajectories. If we integrate these two trajectories simultanetely, the distance between two corresponding points (one on each trajectory) does not remain infinitesimally small (it increases exponentially with time until the two trajectories are practically uncorrelated). For example, one of the two trajectories coming from the region D_0 would go to D_1 while the other one would go to D_{-1}. In Fig.10 we show the time series coresponding to the trajectories T_1 and T_2 (dash line) starting from (0.001,0.001,0.001) and (0.0015,0.001,0.001), respectively .The two trajectories are close to each other until $t = 280$ when T_1 and T_2 are both in the middle region D_0. Then T_1 goes to the region D_1 while T_2 returns to D_{-1}. After this, T_1 and T_2 are completely uncorrelated.

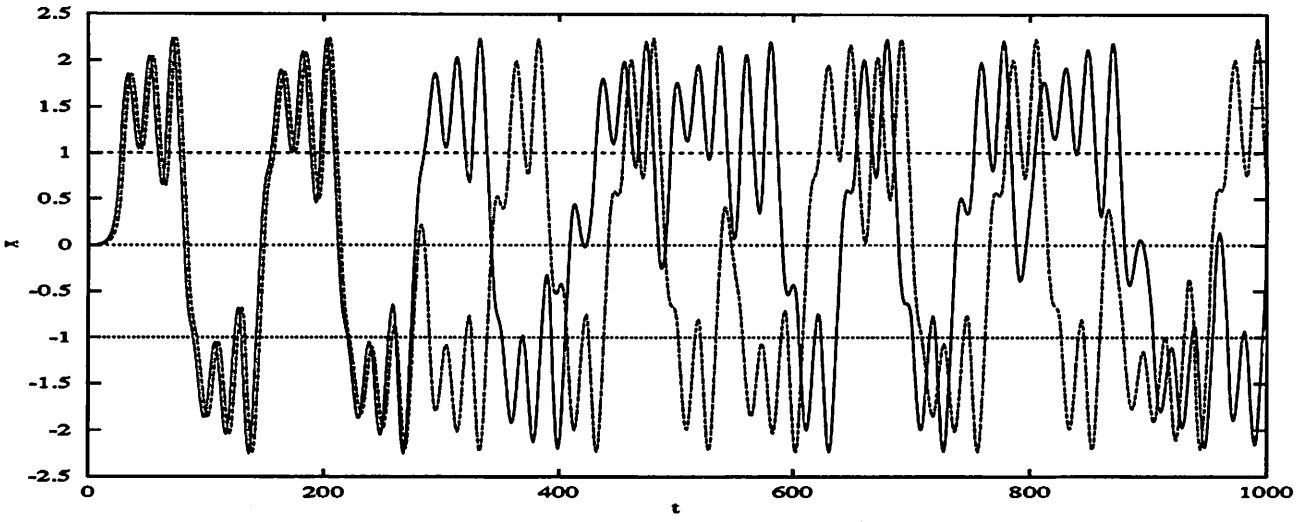

Figure 10: Two time series of the double scroll attractor obtained from Σ_d, starting from two different but close initial conditiions

3.2.3 The double hook attractor

For $\tilde{\alpha} = 9, \tilde{\beta} = 14.28, \tilde{m}_0 = -1/7$, and $\tilde{m}_1 = 2/7$, (36) has a chaotic attractor [16], as shown in Fig 11. This corresponds to the following set of eigenvalues :

$$\begin{cases} \mu_1 = 1.15 & \mu_2 = -2.98 & \mu_3 = -5.70 \\ \nu_1 = -0.89 & \nu_2 = 0.15 + j1.00 & \nu_3 = 0.15 - j1.00 \end{cases} \tag{42}$$

This eigenvalue pattern is of *Type I*. In the middle region, instead of having one real eigenvector and an eigenplane as it was the case so far, there are three real eigenvectors. Two of them are stable and the third one is unstable. The Jordan form of the Jacobian matrix of the linear dynamical system present in D_0 is a diagonal matrix with the eigenvalues on its diagonal. The associated dynamical system has a solution of the type :

$$\begin{cases} x = Ge^{\mu_1 t} \\ y = He^{\mu_2 t} \\ z = Ke^{\mu_3 t} \end{cases} \tag{43}$$

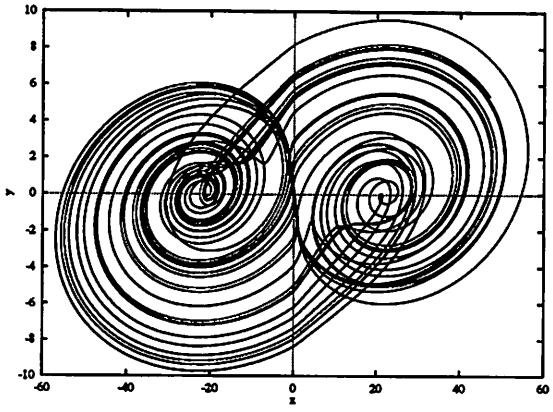

Figure 11: Phase portrait of the double hook attractor obtained from Σ_d

3.3 Two examples of attractors from Chua's torus circuit

The dimensionless form of Chua's torus circuit [17] is

$$\begin{cases} \frac{dx}{dt} &= -\alpha \hat{f}(y-x) \\ \frac{dy}{dt} &= -\hat{f}(y-x) - z \\ \frac{dz}{dt} &= \beta y \end{cases} \tag{44}$$

3.3.1 A two-dimensional quasi-periodic torus

For $\tilde{\alpha} = 2, \tilde{\beta} = 1, \tilde{m_0} = 0.1$, and $\tilde{m_1} = -0.07$, (44) leads to a quasi-periodic 2-torus [12] [17], as shown in Fig 11-a . It corresponds to the following set of eigenvalues :

$$\begin{cases} \mu_1 = 0.1955 & \mu_2 = -0.04794 + j1.004 & \mu_3 = -0.04794 - j1.004 \\ \gamma_1 = -0.1381 & \nu_2 = -0.03419 + j1.00 & \nu_2 = -0.03419 - j1.00 \end{cases} \tag{45}$$

This is equivallent to :

$$\begin{cases} p_1 = 0.09958 & p_2 = 0.9917 & p_3 = 0.1975 \\ q_1 = -0.06970 & q_2 = 0.9917 & q_3 = -0.1382 \end{cases} \tag{46}$$

We cannot apply (11) or (18) to obtain the parameters of Σ_c and Σ_d because the eigenvalue pattern belongs to S_c and S_d. One can check that equation (14), (15) and (22) are satisfied by (46). As it has been explained earlier, we shall have to perturb the eigenvalues in order to use Chua's oscillator to obtained the attractor shown in Fig. 12. Let us add for example 10^{-6} to μ_1 and obtain the following perturbated values for the parameters of Chua's oscillator (resp. Chua's oscillator dimensionless equations) :

$C_1 = 1$; $C_2 = 22.67 \times 10^8$; $G = -47421$; $G_a = 47421$; $G_b = 47421$; $L = 210^{-10}$; $R = 0.0$

(resp. $\alpha = 22.67 \times 10^8$; $\beta = 47.42 \times 10^8$; $\gamma = -0.7175$; $m_0 = -0.9999$; $m_1 = -1.0000$; $k = -1$)

Unfortunately, when we integrate the system Σ_d, with our program, we do not find the trajectory shown in Fig.11-a, because the calculations are not made with enough precision. After our perturbation of μ_1, K_1 and K_3 defined in (12) are not equal to zero any more, they are 1.2×10^{-5} and 6.7×10^{-6} respectively. These coefficient are different from zero, but they remain small. Let us try to perturb the eigenvalues a little bit more. We now add 10^{-2} to μ_1. In this case, we find :

$C_1 = 1$; $C_2 = 31.553$; $G = -5.572$; $G_a = 5.531$; $G_b = 5.701$; $L = 0.01581$; $R = 0.001866$

(resp. $\alpha = 31.553$; $\beta = 64.257$; $\gamma = -0.6683$; $m_0 = -0.9926$; $m_1 = -1.0230$; $k = -1$)

With these parameters, using Σ_d, we obtain the trajectory shown in Fig.12-b. One can verify that it is identical to that obtained directly from the torus circuit shown in Fig.12-a.

[12] see 5.3 for a definition

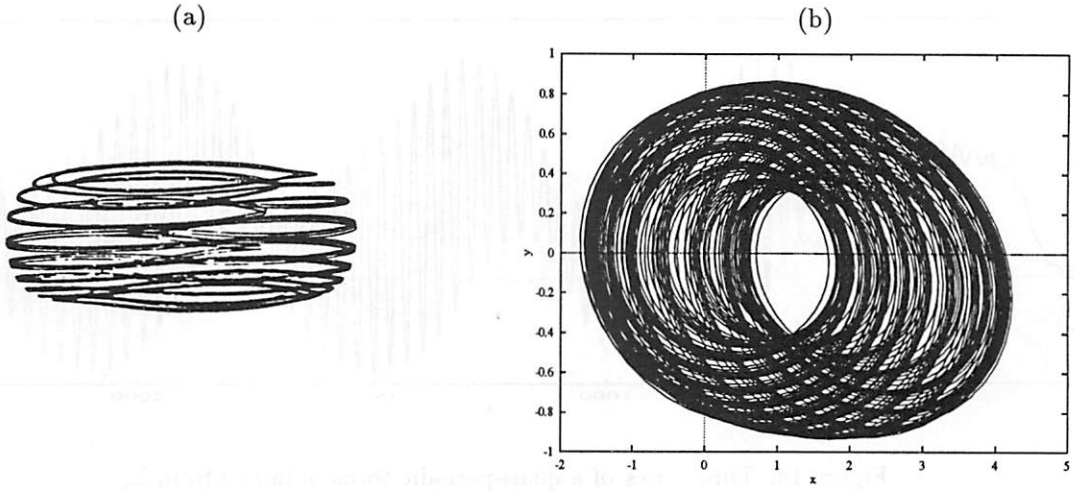

Figure 12: Two-dimensional quasi-periodic torus obtained from (a) the original Chua's torus system and from (b) Σ_d

.

Figure 13: Typical trajectories and eigenspaces for the 2-torus

As we did for the double scroll, let us also examine the typical trajectories and the associated eigenspaces represented in Fig.11 . The eigenvalue pattern is also of type (c) in the middle region, and of type (b) in the outer region. However, there are two slight differences :

- The magnitude of $|\gamma_1| = 0.14$ is not as large as for the double scroll (1.29) and therefore the "flattening" onto $E^U(P^{\pm})$ is relatively weak.

- $E^S(0)$ and $E^U(P^{\pm})$ are almost parallel to each other.

The reader can verify that if we increase $(\tilde{\alpha})$ further, we would evenetually find a double scroll $(\tilde{\alpha} = 30)$. A time series of the quasiperiodic attractor is given in Fig.11. It is characteristic of a quasi-periodic system with two incommensurate frequencies.

Note that the coefficient obtained after perturbing μ_1 by 10^{-6} would lead to a trajectory identical to that obtained in Fig.11a if our calculations have better precision [13]. The question is : how much can we perturb the eigenvalues and still obtain the same trajectory ? There is no general answer to this question, as it depends on the attractor [14]. We know that in theory, if the perturbation is small enough, we shall find a system that has the same qualitative behavior. In practice, in section 4, we have found without any difficulty

[13] For example, one can verify that in Σ_d we are in fact interested in m_0+1, which is close to 2×10^{-8}. Our program, does not allow us to carry out the calculation with enough precision

[14] see 5.2 for more details

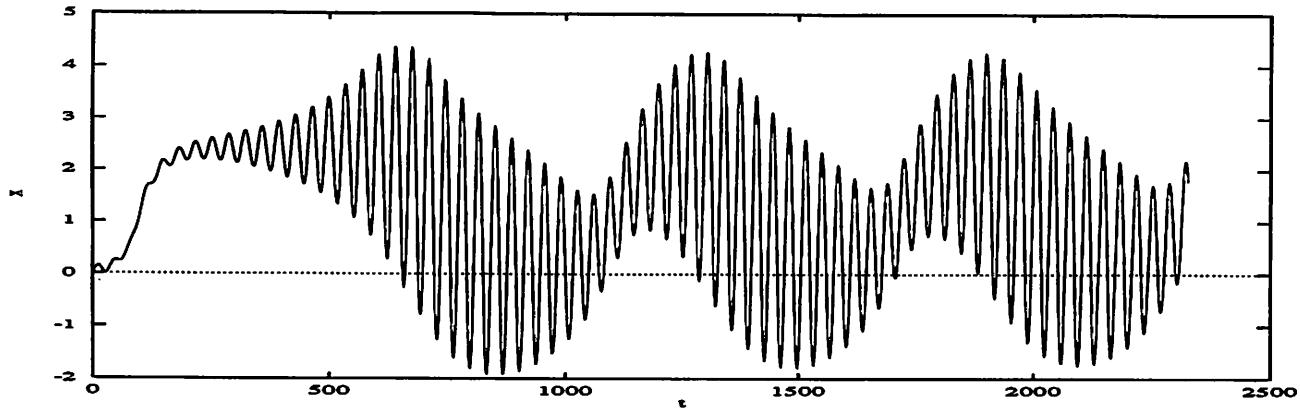

Figure 14: Time series of a quasi-periodic torus obtained from Σ_d

the coefficients of Σ_d, that give the expected trajectory with our program. As we shall see in this section, one must identify where the singularity comes from ($K_1 = 0$ and $K_3 = 0$ in our case) and slightly modify the eigenvalue pattern to avoid the singularity. Note that in our case, by changing one of the eigenvalues we shall exit from S_d, if we change several eigenvalues we should verify that we do not stay inS_d.

3.3.2 A folded torus

For $\tilde{\alpha} = 15, \tilde{\beta} = 1, \tilde{m_0} = 0.1$, and $\tilde{m_1} = -0.07$, (44) has an attractor [17], as shown in Fig 12-a,. It corresponds to the following set of eigenvalues :

$$\begin{cases} \mu_1 = 1.408 & \mu_2 = -0.0161 + j1.006 & \mu_3 = -0.0161 - j1.006 \\ \nu_1 = -0.997 & \nu_2 = 0.01695 + j1.00 & \nu_2 = 0.01695 - j1.00 \end{cases} \tag{47}$$

This is equivalent to :

$$\begin{cases} p_1 = 1.376 & p_2 = 0.9634 & p_3 = 1.425 \\ q_1 = -0.9634 & q_2 = 0.9664 & q_3 = -0.9976 \end{cases} \tag{48}$$

As above, we have to perturb the eigenvalues Let us add 0.01 to μ_1, to obtain the following values of the parameters for Chua's oscillator (resp. Chua's oscillator dimensionless equations) :
$C_1 = 1$; $C_2 = 13.325$; $G = -0.9309$; $G_a = -0.4412$; $G_b = 1.8984$; $L = 0.07214$; $R = 0.004742$
(resp. $\alpha = 13.325$; $\beta = 213.12$; $\gamma = -0.9408$; $m_0 = 0.4740$; $m_1 = 2.0393$; $k = -1$)
Observe that the trajectory shown in Fig.15b is identical to that of Fig.15a.

3.4 Ogorzalek's example

In order to simplify the equations of his ladder circuit, Ogorzalek assumes in [18] that $R_1 = R_2 = R_3 = 1\Omega$ and $C_1 = C_2 = C_3 = 1F$. The state equation becomes :

$$\begin{pmatrix} \dot{x_1} \\ \dot{x_2} \\ \dot{x_3} \end{pmatrix} = \begin{pmatrix} -2 & 1 & 0 \\ 1 & -2 & 1 \\ 0 & 1 & -1 \end{pmatrix} \begin{pmatrix} x_1 \\ x_2 \\ x_3 \end{pmatrix} + \begin{pmatrix} 1 \\ 0 \\ 0 \end{pmatrix} \tilde{f}(x_3) \tag{49}$$

For $m_0 = -33.03$ and $m_1 = 400$, Ogorzalek obtains the trajectory shown in Fig.13-a . The eigenvalue pattern of this system is :

$$\begin{cases} \mu_1 = -0.809 & \mu_2 = 0.00753 + j0.4045 & \mu_3 = 0.00753 - j0.4045 \\ \nu_1 = 0.9234 & \nu_2 = -0.8588 + j1.00 & \nu_3 = -0.8588 - j1.00 \end{cases} \tag{50}$$

this is equivalent to :

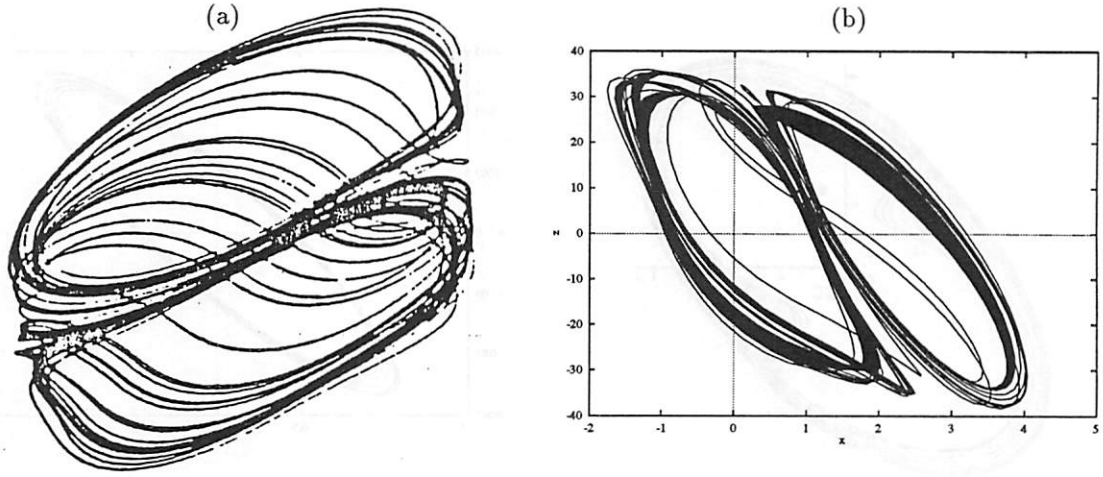

Figure 15: Folded torus obtained from (a) the original Chua's torus system, and (b) from Σ_d.

$$\begin{cases} p_1 = -0.794 & p_2 = 0.151 & p_3 = -0.132 \\ q_1 = -0.794 & q_2 = 0.151 & q_3 = 1.604 \end{cases} \tag{51}$$

Observe that since $p_1 = q_1$, we have to perturb the eigenvalue pattern in order to be able to determine the parameters of Σ_c and Σ_d. If we modify one of the eigenvalues, it will have an effect on p_1 or q_1 and therefore we shall be able to calculate the parameters of Σ_c and Σ_d. In the case of the torus we have seen that if the perturbation is too small the parameters exist but in practice for numerical reasons the integration of the system does not lead to the expected trajectory. On one hand, we want to avoid a singularity of the type $\frac{1}{p_1 - q_1}$. On the other hand, we do not want to change the eigenvalues too much because then it is very likely that we shall not find the same qualitative behavior. The best way to find a numerically appropriate pertubation is to modify $(p; q)$ directly, instead of $(\mu; \nu)$. By proceeding this way we are sure that we eliminate the singularity as efficiently as possible for a minimum perturbation of the eigenvalues. In our case, let us add 0.1 to p_1 and substract 0.1 from q_1, in order to maximize $p_1 - q_1$. This leads to the following eigenvalue pattern :

$$\begin{cases} p_1 = -0.694 & p_2 = 0.151 & p_3 = -0.132 \\ q_1 = -0.894 & q_2 = 0.151 & q_3 = 1.604 \end{cases} \tag{52}$$

which is equivalent to :

$$\begin{cases} \mu_1 = -0.746 & \mu_2 = 0.00926 + j0.431 & \mu_3 = 0.00926 - j0.431 \\ \nu_1 = 0.918 & \nu_2 = 0.922 + j1.00 & \nu_2 = -0.922 + j1.00 \end{cases} \tag{53}$$

and to the following parameters for chua's oscillator (resp dimensionless equations)

$C_1 = 1$; $C_2 = -90.364$; $G = 70.549$; $G_a = -69.769$; $G_b = -69.737$; $L = 0.0002037$; $R = 0.0001590$

(resp. $\alpha = -90.364$; $\beta = -89.114$; $\gamma = -1.000$; $m_0 = -0.98893$; $m_1 = -0.98848$; $k = -1$)

The trajectories on Fig. 16a and Fig. 16b do not look quite the same. This is however only an illusion. As shown in Fig. 16c, the illusion is caused by the geometry because in this example, the trajectory is flattened onto a plane P that does not correpond to any of the planes $x = 0$, $y = 0$ or $z = 0$. Therefore there is no way of expending the trajectory along one of the axes. However, as shown in Fig. 16d-e, if we rotate the attractor around the y-axis through an angle of 44.6 degrees to expose the third dimension of the attractor in greater details, we would eventually obtain the attractor shown in Fig. 16f that looks identical to the original one in Fig. 16a.

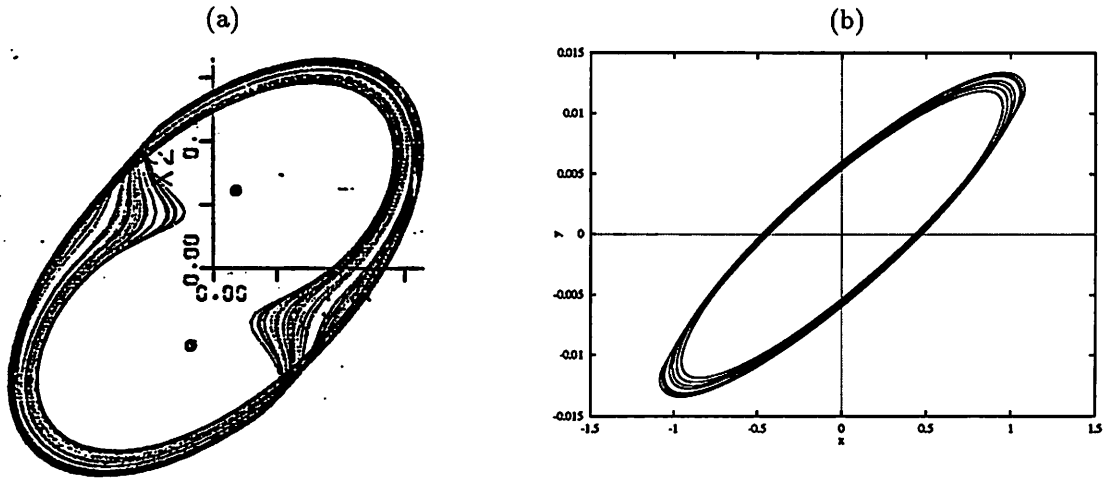

Figure 16: Attractor from Ogorzalec's example obtained from (a) the original system and from (b) Σ_d.

3.5 Brockett's example

In [19], Brockett studies the following single loop feedback system:

$$\begin{pmatrix} \dot{x_1} \\ \dot{x_2} \\ \dot{x_3} \end{pmatrix} = \begin{pmatrix} 0 & 1 & 0 \\ 0 & 0 & 1 \\ -1 & -1.25 & 0 \end{pmatrix} \begin{pmatrix} x_1 \\ x_2 \\ x_3 \end{pmatrix} + \begin{pmatrix} 0 \\ 0 \\ 1 \end{pmatrix} \tilde{g}(x_1) \tag{54}$$

where :

$$\tilde{g}(y) = \begin{cases} -\tilde{k}y & \text{if } |y| < 1 \\ 2\tilde{k}y - 3\tilde{k} & \text{if } 1 < |y| < 3 \\ -3\tilde{k}\ sgn(y) & \text{if } |y| > 3 \end{cases} \tag{55}$$

The only interest of the region $|y| > 3$ is to claim that all solutions of (57) are bounded when t goes to infinity [20]. This region does not play any role in the dynamics of the system, therefore we replace the function $\tilde{g}$ by f defined by $m_0 = -\tilde{k}$ and $m_1 = -3\tilde{k}$. The numerical integrations are conducted for $\tilde{k} = 1.8$.

The phase portrait obtained in [19] from (57) is shown in Fig. 17-a. As in the previous case, we find $p_1 = q_1$, after adding 0.05 to p_1 and subtracting 0.05 from q_1 we obtain :

$$\begin{cases} p_1 = -0.95 & p_2 = 1.25 & p_3 = 1.8 \\ q_1 = -1.05 & q_2 = 1.25 & q_3 = -3.6 \end{cases} \tag{56}$$

this is equivalent to :

$$\begin{cases} \mu_1 = 0.500 & \mu_2 = -0.576 + j0.913 & \mu_3 = -0.576 - j0.913 \\ \nu_1 = -1.12 & \nu 2 = -0.201 + j1.00 & \nu 3 = -0.201 - j1.00 \end{cases} \tag{57}$$

and to the following parameters for Chua's oscillator (resp dimensionless equations)
$C_1 = 1$; $C_2 = 52.056$; $G = -36.003$; $G_a = 36.656$; $G_b = 36.724$; $L = 0.0007397$; $R = .0005116$
(resp. $\alpha = 52.056$; $\beta = 54.290$; $\gamma = -1.00$; $m_0 = -1.01812$; $m_1 = -1.02003$; $k = -1$)

3.6 Sparrow's example

Sparrow studies in [21] the following system of single-loop feedback system :

$$\begin{cases} \dot{x} = \tilde{g}(z) - x \\ \dot{y} = x - y \\ \dot{z} = y - z \end{cases} \tag{58}$$

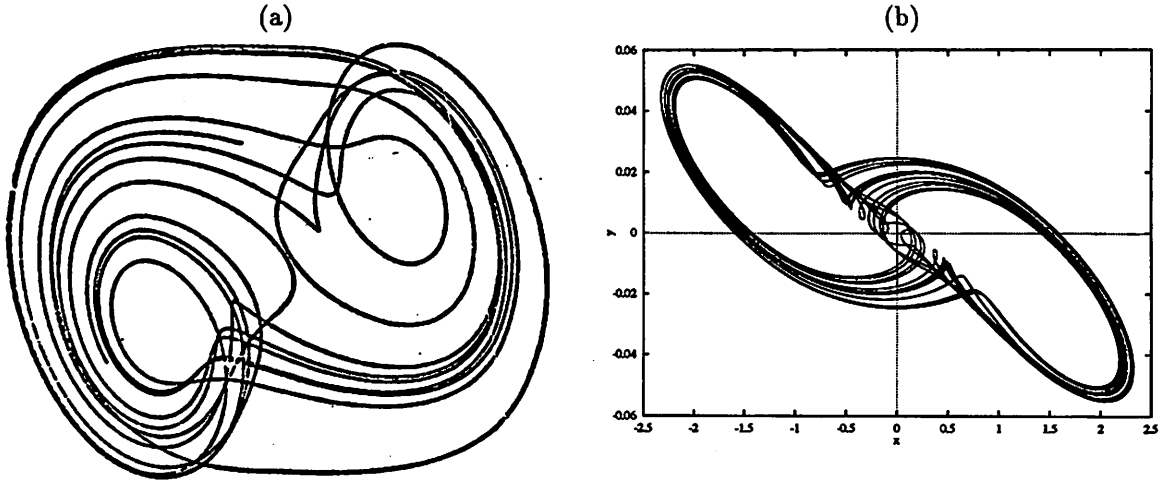

Figure 17: Attractor from Brockett's example obtained from (a) the original system, and from (b) Σ_d.

where:

$$\tilde{g}(z) = \begin{cases} = & -8.14z & +3.35 & \text{if } z \leq \frac{3}{7} \\ = & 8.14rz & -0.25 - 3.6r & \text{if } z > \frac{3}{7} \end{cases} \tag{59}$$

This system does not directly belong to $\mathcal{C}$ but after making the system symmetrical with respect the origin, Sparrow obtained the double sided attractor shown in Fig. 18a. The only thing that change in the vector field is the nonlinear function that becomes $\tilde{f}$ given in (35) with $m_0 = -8.4$ and $m_1 = 8.4r$. The numerical integrations are conducted for r=19. After adding 0.1 to p_1 and substracted 0.1 from q_1 we obtained the following eigenvalue pattern:

$$\begin{cases} \mu_1 = 0.677 & \mu_2 = -0.304 + j0.901 & \mu 3 = -0.304 - j0.901 \\ \nu_1 = -1.22 & \nu_2 = -0.304 + j1.00 & \nu_3 = -0.304 - j1.00 \end{cases}$$

and the following parameters for Chua's oscillator (resp. Chua's dimensionless oscillator equations):
$C_1 = 1$; $C_2 = -100.1$; $G = 62.019$; $G_a = -61.40$; $G_b = -61.35$; $L = 0.0002635$; $R = 0.0001631$
(resp. $\alpha = 100.18$; $\beta = -98.823$; $\gamma = -1.00$; $m_0 = -0.99002$; $m_1 = -0.98933$; $k = -1$)
This leads to the trajectory shown in Fig. 18b. For the same reasons as in the case of Ogorzalec's example, we do not obtain a trajectory similar to that in Fig. 18a. However, after a rotation around the x-axix through an angle of 44.6 degrees, we find the trajectory shown in Fig. 18c. Observe that the attractor has the same geometrical structure as that obtained from Ogorzalec's example. Although these two systems have different eigenvalue patterns, the structure of the attractors is the same. We had already seen in section 3.4 that it is not always obvious to recognize that two attractors have the same geometrical structure, but it is not always obvious either that two attractors have different geometrical structures. In the next section where we present a gallery of attractors, we have checked carefully that this is not the case.

3.7 Conclusion

For each example considered in this section, it has been possible to find easily the parameters for both Chua's oscillator and of its dimensionless equations that lead to the same behavior. Through these examples, we have also presented a method to perturb the eigenvalues when needed. This method can be used to map the dynamics of any system of $\mathcal{C}$ into that of Σ_c or Σ_d, as soon as we know its eigenvalue pattern. The reader can directly use the program provided with this article, or Chua's oscillator to study the dynamics of any element of $\mathcal{C}$. In the next section, we shall give a list of all the attractors discovered so far in $\mathcal{C}$.

4 A gallery of attractors

In this section, we present a zoo of attractors obtained from elements of Chua's canonical family. As it has already been explained earlier, all these attractors lie in the dynamics of Chua's oscillator and in that of

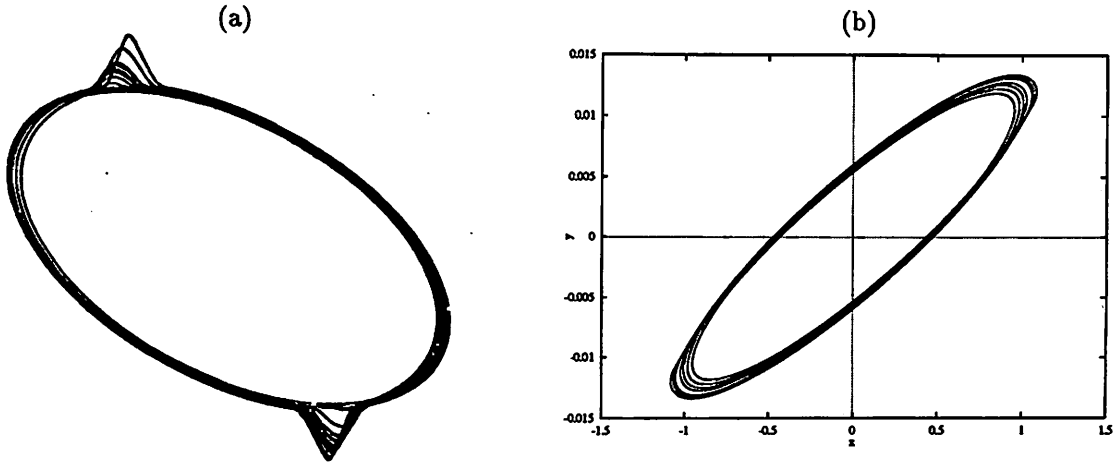

Figure 18: Attractor from Sparrow's example obtained from (a) the original system and from (b) Σ_d.

its associated dimensionless form. We shall use this last system Σ_d to generate the trajectories of each of them. For each attractor, we shall also provide the eigenvalue pattern, the parameters of Chua's oscillator dimensionless equations Σ_d, as well as the Lyapunov dimension [15] [16] . All of these information are gathered in a table given in appendix B.

Among this zoo of attractors, we first find those studied in the previous section : Rossler's attractor, the double scroll attractor, the double hook attractor, the quasi-periodic and folded tori, and the Ogorzalec, Brockett and Sparrow's examples. In the case of Chua's circuit we present six new attractors. In addition to the attractors originally discovered from one of the system presented in the previous section, we add 12 other attractors reported in Chua's oscillator.

4.1 Attractors obtained from Chua's circuit

In addition to the R*ddotos*sler's attractor, the double scroll attractor, and the double hook attractor, we add six other attractors obtained from Chua's circuit[17] :

- a torus obtained for large values of $\tilde{\alpha}$ and $\tilde{\beta}$.[18] : $\tilde{\alpha} = 1800.0; \tilde{\beta} = 10000.0; \tilde{m}_0 = -1.026; \tilde{m}_1 = -0.982$ and of course as it has already been explained in section 3.2, $\gamma = 0$.

- three attractors obtained for the following values of parameters for the dimensionless form of Chua's circuit :

$\tilde{\alpha} = -4.087; \tilde{\beta} = -2.0; \tilde{m}_0 = -1.1429; \tilde{m}_1 = -0.7142$ (Fig. 19b)

$\tilde{\alpha} = -6.691; \tilde{\beta} = -1.520; \tilde{m}_0 = -1.1429; \tilde{m}_1 = -0.7142$ (Fig. 19c)

$\tilde{\alpha} = 8.342; \tilde{\beta} = 11.925; \tilde{m}_0 = -1.146; \tilde{m}_1 = -0.8533$ (Fig. 19d)

- Two attractors obtained for the same values of parameters but different initial conditions. One of them is not symmetrical with respect to the origin, therefore we can consider its symmetric image as a third attractor. These attractors are obtained for : $\tilde{\alpha} = 15.6, \tilde{\beta} = 28.58, \tilde{m}_0 = -8/7$, and $\tilde{m}_1 = -5/7$ and the following initial conditions (for Σ_d):

$x = 0.1; \quad y = 0.1; \quad z = 0.1;$ (Fig. 19e)

$x = 1.163764; \quad y = -0.09723353; \quad z = -.90565;$ (Fig. 19f)

$x = -1.163764; \quad y = 0.0972335; \quad z = .90565;$ (the symmetric image of the previous one)

The theory of confinors [22] [23] made it possible to prove rigorously that these three attractors are different. As we shall see in the next section, this is a non-trivial problem that will not be tackled in this

[15] see 5.4

[16] obtained with the software package INSITE

[17] as it has been explained in section 3.2 the coefficients of Chua's oscillator are immediately obtained from those of Chua's circuit

[18] Note that it is the first torus obtained in Chua's circuit

paper. Let us say that all the geometrical structure of the attractors discovered so far in $\mathcal{C}$ is close to that of one of the attractors presented in our gallery.

4.2 Concluding remarks

As explained earlier in this paper, all of the dynamics of $\mathcal{C}$ lie in a five-parameter family of dynamical system : Σ_d. The corresponding five-dimensional parameter space P_d is huge and a systematic scanning of P_d is almost impossible. So far, only a tiny portion of P_d has been explored, many more new attractors are expected. The aim of this gallery is mainly to give an idea of the wealth of the complicated dynamics in $\mathcal{C}$ and to encourage the reader to look for new attractors with programs like that proposed in this article or that in [24]. Note that knowing the five coefficients of Σ_d one can use (5) backwards to determine the seven circuit parameters of Σ_c. There are two degrees of freedom in this process, the reader can take advantage of them to choose values of the circuit parameters most convenient for its own implementation of Chua's oscillator. Equation (11) could also be directely applied.

Figure 19: Attractors originally obtained from Chua's circuit

Figure 20: Some other attractors obtained from Chua's oscillator

5 Elements of dynamics in $\mathcal{C}$

5.1 Comparison of the original system and the corresponding Chua's canonical systems Σ_c and Σ_d

Let us first recall the exact relation between the original dynamical system and that obtained from Chua's oscillator Σ_c or from its associated dimensionless system Σ_d. Let us denote by F_o,F_c and F_d the vector field of the original circuit, that of Σ_c, and Σ_d, respectively. As it is proven in section 6, there exists two invertible matrices J_c and J_d, and a positive non-zero constant S_d, such that[19]:

$$\begin{cases} F_c = J_c^{-1} F_o J_c \\ F_d = S_d J_d^{-1} F_o J_d \end{cases} \tag{60}$$

If $X(t, x_0)$ is a solution of the original equation

$$\dot{X}(t) = F(X) \tag{61}$$

where t is the time and x_0 the initial condition (i.e. the value of X at $t = 0$), then

$$\dot{\overline{J_c X(t)}} = J_c \dot{X} = J_c F_c(X) = F_c(J_c X(t)) \tag{62}$$

and

$$\dot{\overline{J_d X}} = J_d \dot{X} = S_d J_d F_d(X) = S_d F_d(J_d X(t)) \tag{63}$$

Equation (62) implies that $J_c X(t)$ is a solution of Σ_c, and (63) implies that $J_d X(S_d t)$ is a solution of Σ_d. This means that the trajectory obtained from Chua's canonical circuit is the same as X(t), but in a different basis. The trajectory obtained from Chua's canonical equation is also the same as $X(t)$ in a different basis, but after a time rescaling [20]. Therefore, we have to compare two trajectories which are not in the same basis.

[19] J and J_c are said to be linearly conjugate, while J and J_d are said to be linearly equivalent

[20] Note that we cannot see this time rescaling in a phase portrait

If there exists a relation of the type (60) between two vector fields (after a small perturbation if needed) the two systems are said to have the same qualitative behavior. In section 3, we did not insist on this point. By choosing the appropriate view point, we were able to verify that the trajectories obtained from the original system and from Σ_d look the same. Regardless of this, strictly speaking, we had not the same trajectory in two different basis, but two different trajectories. Indeed, we should not think in term of trajectory but in term of attractor as we explain below.

5.2 Steady-state behavior and attracting sets

Let us first give some definitions:

A steady state refers to the asymptotic behavior as $t \rightarrow \infty$.

A point y is a limit point of x if, for every open neighborhood U of y, $X(t,x)$ repeatedly enters U as $t \rightarrow \infty$.

The set of all limit points of x is called the limit set of $X(t,x)$.

A limit set L is said to be *attracting* if there exists an open neighborhood of L such that the steady-state of $X(t,x)$ is L for any x of U.

The *basin of attraction* of an attracting set L is $B(L)$ such that every trajectory starting from $B(L)$ tends toward L as $t \rightarrow \infty$.

Attracting limit sets are the only set that can be observed in physical systems. This does not mean that a nonattracting set cannot have an influence on the transient (before the steady-state is reached). The definition of limit sets that we gave is in fact too simple for complex steady-state behaviors such as those existing in chaotic systems. The term *strange attractor* has been introduced as the set on which the trajectory accumulates. For us we shall use interchangeably attracting limit set and attractor. Note that in a stable linear system there is only *one* limit set but in a nonlinear system there are typically several attracting sets with their own basins of attraction. The initial conditions determine in which limit set the system settles.

5.3 Equilibrium points, periodic orbits, quasi-periodic orbits and chaos

X_{eq} is an *equilibrium point* if for all t: $X(t, X_{eq}) = X_{eq}$.

$X(t, X_0)$ is a *periodic solution* if there exists a minimal period T such that $X(t, X_0) = X(t+T, X_0)$ for all t.

$X(t, X_0)$ is a *quasi-periodic* solution if it can be written as the sum of periodic functions : $X(t) = \sum_i h_i(t)$ where h_i has a minimal period T_i and a frequency f_i. In addition to this, there exists a finite set of base frequencies $(\hat{f}_1, ..\hat{f}_p)$ such that

- there does not exist a nonzero set of integers $(\hat{k}_1, ..\hat{k}_p)$ such that $\hat{k}_1\hat{f}_1 + .. + \hat{k}_p\hat{f}_p = 0$
- it forms a finite integral basis for any f_i.

The base frequency is not unique but p is. A quasi-peiodic solution with p base frequencies is called *p-periodic.*

From a practical point of view, *chaos* can be defined as none of the above; that is, a bounded steady-state behavior that is not an equilibrium point, not periodic, and not quasi-peiodic. The limit set for chaotic behavior is not a simple set like a circle or a torus but it is related to fractals and Cantor sets [25].

Another property of chaotic system is its *sensitive dependence on initial conditions* already mentioned in section 3.2.2. Consider two different initial conditions arbitrarily close to each other, the trajectories corresponding to these two points diverge at a rate characteristic of the system before becoming uncorrelated for all practical purposes. Even if two different initial conditions are very close to each other, so that they cannot be distinguished, the corresponding trajectories will diverge and become uncorrelated after a finite amount of time. Therefore, no matter how precisely the initial conditions are known, the long term behavior of a chaotic system cannot be predicted. That is why chaotic systems, although deterministic, are said to exhibit a "random behavior". This is the reason why it is impossible to reproduce with Chua's canonical system exactly the same trajectory as with the original system. In the previous section, we in fact verified that the attractors obtained from the original system from Σ_d look the same. The reader can easily imagine that to prove that two chaotic attractors are identical, or different, is a non trivial task [23]. When we do not have to perturb the parameters, the dynamical systems Σ_o, Σ_c and Σ_d are equivalent. Therefore the same

attractors should be present in the three systems. In fact this is not obvious either. Indeed the vector fields are not defined with infinite precision. Fortunately, except in some pathological cases, attractors are said to be stucturally stable which means that they are preserved under perturbations of the system (otherwise we could not see them). This is equivalent to the continuity property of the ODE with respect to parameters. One can also refer to a real circuit where the components are not defined with an infinite precision, but still give birth to the "same" attractor. Assuming that an attractor is stable, it has an open basin of attraction. On one hand, we cannot reproduce the same initial conditions in Chua's canonical systems (Σ_c and Σ_d) as in the original system. On the other hand, it is possible to start in the same basin of attraction and therefore obtain the same attractor. That is what we did in the previous section. Also note that if the notion of the attractor is a non-trivial one, then it is not obvious either to determine whether or not two attractors are distinct, if their bassins of attraction are distinct. In this paper we shall not tackle this problem. In the previous section, we do not pretend to have given an exhaustive list of all the existing attractors in Chua's canonical circuit but rather that all the attractors discovered so far in $\mathcal{C}$ have a geometrical structure close to that of one presented in the gallery. There are in fact many attractors present, thinking for example of a bifurcation sequence where the attractors evolve, merge, etc... [13] [26]. We have also seen in section 3.4 that it is not always easy to recognize that two attractors are similar. To build a complete list of attractors, it would be at the same time difficult to be exhaustive but also to make sure not to list the same attractor twice. In addition to the phase portrait, one of the criteria to characterize an attractor is its Lyapunov exponents.

5.4 Lyapunov exponents

After this brief presentation of what chaos is, we introduce a generalization of the eigenvalues at the equilibrium points. The Lyapunov exponents are used to determine the stability of any asymptotic behavior (behavior when $t \rightarrow \infty$) including chaotic and quasi-periodic solution for which they provide valuable information. They are defined in the terms of solutions of the variational equation as follows: let $\{m_i(t)\}_{i=1}^3$ be the eigenvalues of the Jacobian matrix of $F(X)$ evaluated at $X = X(t, X_0)$. The Lyapunov exponents are defined by :

$$\lambda_i = \lim_{t \rightarrow \infty} \frac{1}{t} ln|m_i(t)| \tag{64}$$

if the limit exists [21]. To have a better understanding of what these Lyapunov exponents are, let us for example find them at the equilibrium point P_+. The eigenvalues of the Jacobian matrix M_1 are $\mu_i(t)_{i=1}^3 = e^{\mu_i(t)}$. Therefore :

$$\begin{array}{rcl} \lambda_i & = & \lim_{t \rightarrow \infty} \frac{1}{t} ln|m_i(t)| \\ & = & \lim_{t \rightarrow \infty} \frac{1}{t} Re[\mu_i]t = Re[\mu_i] \end{array} \tag{65}$$

Hence, in this special case, the Lyapunov exponents are equal to the real part of the eigenvalues at the equilibrium point; they indicate the rate of contraction ($\lambda_i < 0$) or expansion ($\lambda_i > 0$) near the equilibrium point.

Suppose that $x_0 \neq P_+$ but $X(t, x_0) \rightarrow P_+$ as $t \rightarrow \infty$, which means that x_0 is in the basin of attraction of P_+. Since the Lyapunov exponents are defined as the limit as $t \rightarrow \infty$, the Lyapunov exponents of x_0 and P_+ are identical. In general, every point of an attractor has the same Lyapunov exponents as the attractor [22]; therefore we can refer to the Lyapunov exponents of an attractor. It is proven in dimension n that at least one of the Lyapunov exponents must be equal to zero. In addition to this , note that for an attractor, the contraction must outweight expansion so :

$$\sum_{i=0}^{n} \lambda_i < 0 \tag{66}$$

From these Lyapunov exponents :

$$\lambda_1 \geq \lambda_2 \geq ....\lambda_n \tag{67}$$

[21] *lim* can be replaced by *lim sup* to guarantee existence of the Lyapunov exponents. Our short presentation is only true when the limit exists.

[22] We should say for almost every point in some cases of strange (or chaotic) attractors, but it is always true for non-strange attractors

Kaplan and Yorke defined the Lyapunov dimension as :

$$D_L = j + \frac{\lambda_1 + \lambda_2 + \lambda_j}{\lambda_{j+1}} \tag{68}$$

where j is the largest integer such that $\lambda_1 + \lambda_2 + \lambda_j \geq 0$.

5.5 Classification of Attracting sets

Having now a better idea of what attractors are, let us classify them. One of the features of chaos is its sensitive dependence on initial conditions. This occurs only in an expanding flow. Hence, what distinguishes a chaotic (or strange) attractor from the other types of attractor is the presence of at least one positive Lyapunov exponent. In the three-dimensional case, we can only have one positive Lyapunov exponent [23] but in systems of higher dimension, it is possible to have more than one positive Lyapunov exponent; the system is then termed *hyper chaotic*. Among the attracting sets, it is possible to classify these sets as follows:

Classification of attracting sets			
Steady-state	Attracting set	Lyapunov exponents	Lyapunov dimension
Equilibrium point	point	$0 > \lambda_1 \geq ...\lambda_n$	0
Periodic	closed curve	$\lambda_1 = 0;\ 0 > \lambda_2 \geq ...\lambda_n$	1
Quasi-periodic	K-torus	$\lambda_1 = 0 = ... = \lambda_K = 0; 0 > \lambda_{K+1} \geq ...\lambda_n$	K
Chaotic	Cantor-like	$\lambda_1 > 0; \sum \lambda_i < 0$	noninteger

6 Linear conjugacy of two systems having the same eigenvalue pattern

Our aim in this section is to prove the following proposition :

- Two elements of $\mathcal{C}$, whose vector fields F and F' have the same eigenvalue pattern $(\mu;\nu)$ or $(p;q)$ [24] are linearly conjugate, i.e. : there exists a non-singular matrix H such that:

$$H \circ F = F' \circ H \tag{69}$$

Equation (69) immediately implies that the two dynamical systems associated with F and F' have the same qualitative behavior. If X is a solution of the dynmical system

$$\dot{X} = F(X) \tag{70}$$

in the basis B, then:

$$H\dot{X} = H \circ F(X) = F'(HX) \tag{71}$$

therefore $\hat{X} = HX$ is a solution of :

$$\dot{\hat{X}} = F'(\hat{X}) \tag{72}$$

This means that if (70) leads to a trajectory, (72) leads to a qualitatively similar trajectory [25] in another basis defined from B by H (we invite the reader to verify that this is equivalent to what has been said in section 5.1).

More precisely, in order to prove our proposition, we shall show that any vector field of $\mathcal{C}$ with an eigenvalue pattern $(p;q)$ is linearly conjugate to some vector field F_{pq} ***uniquely*** determined by $(p;q)$. By transitivity, this implies that two vector fields having the same eigenvalue pattern $(p;q)$ are linearly conjugate. The proof is decomposed into three steps :

[23] one is equal to zero, and their sum has to be negative

[24] In this section, it will more convenient to define the eigenvalue patterns by $(p;q)$, let us recall that there exists a bijection between $(\mu;\nu)$ and $(p;q)$

[25] with the restrictions of the previous section

6.1 Step 1

Let us first express the vector field F of any element of C in a form in which our proposition will be easier to prove. First, let us recast the vector field F in a basis $\tilde{B}$ where the equations of the boundary planes are $x = 1$ and $x = -1$, respectively. The vector field F can be expressed in the form [26]:

$$f(X) = \begin{cases} \tilde{B}X + \tilde{c} & \text{for } (< \tilde{W}, X >) < -1 \\ \tilde{A}X & \text{for } | < \tilde{W}, X > | \leq 1 \\ \tilde{B}X - c & \text{for } (< \tilde{W}, X >) > 1 \end{cases} \tag{73}$$

where:
$\tilde{A} = (a_{ij})$ is the Jacobian matrix of F in the middle region, denoted by M_0 in Fig.1.
$\tilde{B} = (b_{ij})$ is the Jacobian matrix of F in the outer region, denoted by M_1 in Fig.1.
$\tilde{c}$=$(c_1.c_2, c_3)$ is a vector of R^3 that ensures the continuity of F on the boundary point.
$\tilde{W} = (1, 0, 0)^T$ is a vector of R^3.

The coordinates of a point belonging to the boundary plane B_1 can be expressed by $(1, y, z)$ where y and z are two real numbers. The assumption that F is continuous on B_1 is equivalent to :

$$\forall y, z \in R, \quad \tilde{A} \begin{pmatrix} 1 \\ y \\ z \end{pmatrix} = \tilde{B} \begin{pmatrix} 1 \\ y \\ z \end{pmatrix} + \tilde{c} \tag{74}$$

which can be explicitly written as follows :

$$\forall y, z \in R, \quad \begin{cases} a_{11} - b_{11} - c_1 + (a_{12} - b_{12})y + (a_{13} - b_{13})z = 0 \\ a_{21} - b_{21} - c_2 + (a_{22} - b_{22})y + (a_{23} - b_{23})z = 0 \\ a_{31} - b_{31} - c_3 + (a_{32} - b_{32})y + (a_{33} - b_{33})z = 0 \end{cases} \tag{75}$$

Eq.(75) implies that the last two columns of the matrices $\tilde{A}$ and $\tilde{B}$ are identical. Thus there exists a vector

$$\tilde{P} = \begin{pmatrix} -b_{11} - c_1 \\ -b_{21} - c_2 \\ -b_{31} - c_3 \end{pmatrix} \tag{76}$$

such that

$$\tilde{B} = \tilde{A} + P(1, 0, 0) \tag{77}$$

Therefore f can be expressed as follows [15] [14] :

$$\begin{aligned} f(X) = \tilde{A}X + \tfrac{1}{2}\tilde{P}\Big(| < \tilde{W}, X > -1| + (< \tilde{W}, X > -1)\Big) \\ - \Big(| < \tilde{W}, X > +1| - (< \tilde{W}, X > +1)\Big) \end{aligned} \tag{78}$$

Let us now note that there exists a nonsingular matrix H such that $A = H\tilde{A}H^{-1}$ is in its Jordan form [27]. The equation of $f(\cdot)$ as defined in (73) in a basis B, becomes

$$\begin{aligned} Hf(H^{-1}X) = H\tilde{A}H^{-1}X + \tfrac{1}{2}H\tilde{P}\Big\{\Big(| < (H^{-1})^T\tilde{W}, X > -1| \\ + (< (H^{-1})^T\tilde{W}, X > -1)\Big) \\ - \Big(| < (H^{-1})^T\tilde{W}, X > +1| \\ - (< (H^{-1})^T\tilde{W}, X > +1)\Big)\Big\} \end{aligned} \tag{79}$$

in a basis B characterized by the coordinate transformation matrix H from $\tilde{B}$ to B. $\tilde{A}$, $\tilde{P}$ and $\tilde{W}$ are transformed into $H\tilde{A}H^{-1}$, $H\tilde{P}$ and $(H^{-1})^T\tilde{W}$, respectively, and denoted by A,P and W. Therefore, we can suppose, without loss of generality that F A is in the form

[26] <, > denotes the vector dot product. If for exmple $x = (x_1, x_2, x_3)^T$ and $y = (y_1, y_2, y_3)^T$ then $< x, y >= x_1y_1 + x_2y_2 + x_3y_3$

$$\begin{aligned} F(X) &= AX + \tfrac{1}{2}P\,(|<W,X>-1| + (<W,X>-1)) \\ &\quad -(|<W,X>+1| - (<W,X>+1)) \end{aligned} \tag{80}$$

where A is in its Jordan form. Note that W is *not* necessarily equal to $(1,0,0)^T$.

6.2 Step 2

In our second step, we shall prove that there exists a basis B' which transforms A into A' and W into W', where A' is in its horizontal companion form [27] :

$$\begin{pmatrix} 0 & 1 & 0 \\ 0 & 0 & 1 \\ r_1 & r_2 & r_3 \end{pmatrix} . \tag{81}$$

and W' is equal to $(1,0,0)^T$. Let us recall that we have assumed above that A is in its Jordan form, where there are four possible cases :

$$(a)\begin{pmatrix} a & 1 & 0 \\ 0 & a & 1 \\ 0 & 0 & a \end{pmatrix} \quad (b)\begin{pmatrix} a & 0 & 0 \\ 0 & b & 1 \\ 0 & 0 & b \end{pmatrix}$$
$$(c)\begin{pmatrix} a & 1 & 0 \\ 0 & b & 0 \\ 0 & 0 & c \end{pmatrix} \quad (d)\begin{pmatrix} a & 0 & 0 \\ 0 & \sigma & -\omega \\ 0 & \omega & \sigma \end{pmatrix}$$

where a,b and c are distinct and $\omega \neq 0$. In each case, we shall make some assumptions regarding the vector W. They correspond to the fact that, as stipulated in the introduction, there is no plane or line parallel to the boundary plane which is invariant under the action of the linear vector field f in the middle region. Let us now examine these four cases :

6.2.1 Case (a)

Assume that $W = (w_1, w_2, w_3)^T$ satisfies $w_1 \neq 0$. W is tranformed by the matrix $w_1 I$ into $W = (1, y, z)^T$ which in turn is tranformed by the matrix :

$$\begin{pmatrix} 1 & y & z \\ 0 & 1 & y \\ 0 & 0 & 1 \end{pmatrix} \tag{82}$$

into $W = (1,0,0)^T$. The matrix A corresponding to Case (a) is invariant under these transformations. Choosing

$$K = \begin{pmatrix} 1 & 0 & 0 \\ a & 1 & 0 \\ a^2 & 2a & 1 \end{pmatrix} \tag{83}$$

A is transformed into :

$$A' = KAK^{-1} = \begin{pmatrix} 0 & 1 & 0 \\ 0 & 0 & 1 \\ 3a & -3a^2 & a^3 \end{pmatrix} \tag{84}$$

and W is transformed into $W' = (K^{-1})^T W = (1,0,0)^T$.

[27] One can easily verify that $r_1 = p_1, r_2 = -p_2$ and $r_2 = p_3$

6.2.2 Case (b)

Assume that $W = (w_1, w_2, w_3)^T$ satisfies $w_1 \neq 0$ and $w_2 \neq 0$. W is tranformed by the matrix

$$\begin{pmatrix} w_1 & 0 & 0 \\ 0 & w_2 & 0 \\ 0 & 0 & w_3 \end{pmatrix} \tag{85}$$

into $W = (1, 1, z)^T$ which in turn is tranformed by the matrix

$$\begin{pmatrix} 1 & 0 & 0 \\ 0 & 1 & z \\ 0 & 0 & 1 \end{pmatrix} \tag{86}$$

into $W = (1, 0, 0)^T$. The matrix A corresponding to Case (b) is invariant under these transformations. Choosing

$$K = \begin{pmatrix} 1 & 0 & 0 \\ a & b & 1 \\ a^2 & b^2 & 2b \end{pmatrix} \tag{87}$$

A is transformed into

$$A' = KAK^{-1} = \begin{pmatrix} 0 & 1 & 0 \\ 0 & 0 & 1 \\ ab^2 & -(2a+b)b & a+2b \end{pmatrix} \tag{88}$$

and W is transformed into $W' = (K^{-1})^T W = (1, 0, 0)^T$.

6.2.3 Case(c)

Assume that $W = (w_1, w_2, w_3)^T$ satisfies $w_1 \neq 0$, $w_2 \neq 0$ and $w_3 \neq 0$. W is tranformed by the matrix

$$\begin{pmatrix} w_1 & 0 & 0 \\ 0 & w_2 & 0 \\ 0 & 0 & w_3 \end{pmatrix} \tag{89}$$

into $W = (1, 1, 1)^T$. The matrix A corresponding to Case (c) is invariant under these transformations. Choosing

$$K = \begin{pmatrix} 1 & 0 & 1 \\ a & b & c \\ a^2 & b^2 & c^2 \end{pmatrix} \tag{90}$$

A is transformed into

$$A' = KAK^{-1} = \begin{pmatrix} 0 & 1 & 0 \\ 0 & 0 & 1 \\ abc & -(ab+bc+ca) & a+b+c \end{pmatrix} \tag{91}$$

and W is transformed into $W' = (K^{-1})^T W = (1, 0, 0)^T$.

6.2.4 Case(d)

Assume that $W = (w_1, w_2, w_3)^T$ satisfies $w_1 \neq 0$ and $w_2^2 + w_3^2 \neq 0$. W is tranformed by the matrix

$$\begin{pmatrix} w_1 & 0 & 0 \\ 0 & w_2 & w_3 \\ 0 & -w_3 & w_2 \end{pmatrix} \tag{92}$$

into $W = (1,1,1)^T$. The matrix A corresponding to Case (d) is invariant under these transformations. Choosing

$$K = \begin{pmatrix} 1 & 1 & 0 \\ a & \sigma & -\omega \\ a^2 & \sigma^2+\omega^2 & -2\omega^2 \end{pmatrix} \tag{93}$$

A is transformed into

$$A' = KAK^{-1} = \begin{pmatrix} 0 & 1 & 0 \\ 0 & 0 & 1 \\ a+2\sigma & -(2a\sigma+\sigma^2+\omega^2) & a(\sigma^2+\omega^2) \end{pmatrix} \tag{94}$$

and W is transformed into $W' = (K^{-1})^T W = (1,0,0)^T$.

6.2.5 Conclusion

In each case, there exists a matrix K such that :

$$A' = KAK^{-1} = \begin{pmatrix} 0 & 1 & 0 \\ 0 & 0 & 1 \\ p_3 & -p_2 & p_1 \end{pmatrix} \tag{95}$$

$$W' = (K^{-1})^T W = (1,0,0)^T \tag{96}$$

6.3 Step 3

The vector field expressed in (80) is defined by A,W and P. We have proven that there exists a basis B' defined by K from $\tilde{B}$ where *simultaneously* A' is in its companion form (completely defined by p_1, p_2 and p_3) and $W' = (1,0,0)^T$. The last unknown is

$$p' = Kp = (e_1, e_2, e_3)^T \tag{97}$$

We are now going to prove that it is also uniquely defined by $(p;q)$. Indeed, from (80), the Jacobian matrix of the vector field in the outer regions is the matrix :

$$B' = p'w'^T + A' = \begin{pmatrix} e_1 & 1 & 0 \\ e_2 & 0 & 1 \\ e_3+p_3 & -p_2 & p_1' \end{pmatrix} \tag{98}$$

Its characteristic polynomial is :

$$\begin{aligned} P(\lambda) \;=\; |\,\lambda I - B\,| \;=\; & \lambda^3 - \lambda^2(p_1+e_1) \\ & +\lambda(e_1p_1+p_2-e_2) \\ & +(e_3+p_3+p_2e_1-p_1e_2) = 0 \end{aligned} \tag{99}$$

but it is also, by definition of q_1, q_2 and q_3,

$$P(\lambda) = \lambda^3 - q_1\lambda^2 + q_2\lambda - q_3 \tag{100}$$

This leads to the following set of equations

$$\begin{cases} e_1 &= q_1 - p1 \\ e_2 &= -q_2 + p_2 - p_1e_1 \\ e_3 &= -q_3 - p_3 - p_2e_1 + p_1e_2 \end{cases} \tag{101}$$

that uniquely defines p'. Therefore, we have exhibited a vector field F_{pq} uniquely determined by p_1, p_2, p_3, q_1, q_2 and q_3 that is linearly conjugate to any element f of L with the same eigenvalue pattern.

7 Conclusion

In this paper, we have shown how rich the dynamics of a huge family of dynamical systems $\mathcal{C}$ are, but also how all these dynamics can be subsumed within that of a simple circuit or of its associated dimensionless form driven by only five parameters. Since the only nonlinearity in the system is a three-segment piecewise-linear function, in each of the three regions the system is affine, thereby making the study of the dynamics easier. With some examples, it has been possible to give some intuitions about the evolution of the trajectory, mainly in terms of the eigenspaces and the eigenvalues, and to introduce the notion of sensitive dependence to initial conditions. The program available with this article constitutes a complement for the study of attractors in a more interactive way and allows a better understanding of the structure of the attractors. This paper is aimed for the non-specialist. We tried to make full use of the simplicity of the structure of the vector fields in $\mathcal{C}$. However, the theory of chaotic dynamics is much more complex than it appears in this paper. The simplicity of the elements of C provides a vehicle for finding an answer to many questions still opened about *chaos*. Reference [25] constitutes a good introduction to chaotics dynamics, [28] will provide the necessary algorithms to study these systems. To close this paper we remark that the elements of Chua's circuit family can be built with standard components, thereby providing a useful real-time complement to their study.

List of Figures

References

[1] L.O. chua M. Komuro and T Matsumoto. The double scroll family. *IEEE Trans Circuits Syst*, 33:1073–1118, 1986.

[2] L.O. Chua. The genesis of chua's circuit. *Arkiv fur elektronik and Ubertragungstechnik*, 46(4):250–257, 1992.

[3] G.-Q Zhong and F. Ayrom. Experimental confirmation of chaos from chua's circuit. *Int. J. Circuit Theory and Applications*, 15(2), 1985.

[4] M. P. Kennedy. Robust op amp realization of chua's circuit. *Frequenz*, 46:66–80, 1992.

[5] Leon O. Chua. A zoo of stange attractors from the canonical chua's circuits. *35th Midwest Symposium on Circuits and Systems*, 1992.

[6] L.O. Chua G.N. Lin. Canonical realization of chua's circuit family. *IEEE Trans Circuits and Syst*, 37(7):885–902, 1990.

[7] Ph. Deregel. Chua's canonical circuit: a tutotial. *Tech. Rep. M92/99, Electronic Research Laborator, UCB/ERL*, 1992.

[8] J. Kocarev A.S. Huang Lj. Karadzinov and L.O. Chua. A catalog of all canonical piecewise-linear circuits belonging to chua's circuit family. *Tech. Rep. M92/80, Electronic Research Laborator, UCB/ERL*, 1992.

[9] R.N. Madan. Observing and learning chaotic phenomena from chua's circuit. *proc. of 35th Midwest Symposium on Circuits and Systems*, 1992.

[10] C.M. Blazquez and E. Tuma. Dynamics of the double scroll circuit. *IEEE Trans. Circuits and Systems*, 37(5):589–593, 1987.

[11] T.S. Parker and L.O. Chua. The dual double scroll. *IEEE Trans. Circuits and Systems*, 34(9):1059–1073, 1987.

[12] T. Matsumoto L.O. Chua and M. Kumoro. Birth and death of the double scroll. *Physica D*, 24:97–124, 1987.

[13] T. Matsumoto L.O. Chua and M. Kumoro. the double scroll bifurcations. *Int. J. Circuit Theory Appl.*, 14(1):117–146, 1986.

[14] T. Matsumoto L.O. Chua and M. Kumoro. the double scroll. *IEEE Trans. Circuits and Systems*, 32(8):589–593, 1985.

[15] T. Matsumoto. A chaotic attractor from chua's circuit. *IEEE Trans. Circuits and Systems*, 21(12):1055–1058, 1984.

[16] P. Bartissol and L.O Chua. The double hook. *IEEE Trans. Circuits and Systems*, 35(12):1512–1522, 1988.

[17] T. Matsumoto L.O. Chua and R. Tokunaga. Chaos via torus breakdown'. *IEEE Trans. Circuits and Systems*, 34(3):240–253, 1987.

[18] M.J. Ogorzalec. Order and chaos in a third order rc ladder network with nonlinear feedback. *IEEE Trans. Circuits and Systems*, 36(9):1221–1230, 1989.

[19] R. W. Brocket. On conditions leading to chaos in feedback systems. *IEEE Trans. Circuits and Systems*, 1982.

[20] R. W. Brockett and J.L. Willems. Frequency domain stability criteria, part. i amd ii. *IEEE trans. on Automatic control*, 10:407–413, 1965.

[21] C. T. Sparrow. Chaos in a three-dimensional single loop feedback system with a piecewise linear feedback function. *J. of mathematical analysis and applications*, 83(1):275–291, 1981.

[22] R. Lozi and S. Ushiki. Cofinors and bounded-time patterns in chua's circuit and the double scroll family. *Int Journal of Bifurcation and Chaos*, 1(1):119–138, 1991.

[23] R. Lozi and S. Ushiki. Coexisting chaotic attractors in chua's circuit. *Int Journal of Bifurcation and Chaos*, 1(4):923–926, 1991.

[24] M.P. Kennedy C.W. Wu S. Pau and J. Tow. Digital signal processor-based investigation of chua's circuit family. *to appear in special issue on Chua's circuit : a paradigm for chaos*, 1993.

[25] J. Guckenheimer and P. J. Holmes. *Nonlinear Oscillations, Dynamical Systems and Bifurcations of Vector Fields.* Springer-Verlag, 1983.

[26] M. Komuro. Bifurcation equations of 3-dimensional piecewise-linear vector fields. *Advanced series in dynamical systems*, 8:113–123, 1990.

[27] G. Strang. *Linear algebra and its applications.* Harcourt Brace Janovich,publisher, 1980.

[28] T. S. Parker and L. O. Chua. *Practical Numerical algorythms for chaotic systems.* Springer Verlag, New york, 1989.

8 Appendix

8.1 Appendix A : Description of the user-friendly program

The aim of this C-program available on PC is to simulate Chua's canonical equations and to display the trajectory, the eigen spaces, the boundary planes, and to rotate them, and to provide the eigenvalues. In this appendix, we give a brief description of the main menu presented at the top of the screen. To have access to any of the following features, click on the corresponding rectangle with the mouse or press the first letter of the option on the keyboard [28]:

Parameters

Choose the values of $\alpha, \beta, \gamma, m_0, m_1$ and k. To set the value of a particular parameter, choose the **parameter** option in the main menu and then select the parameter to be modified by clicking on the appropriate menu button. When the parameter is chosen, a tick mark appears in the box along side the name of the parameter. Enter the parameter value by typing the desired number in the dialogue box and pressing **modify**, or by incrementing/decrementing the digits of the display by clicking on the arrow keys. Note that k can only take the value 1 and -1, by clicking on the button k one sets the opposite value.

The **calculate** button initiates the circuit equations from the chosen initial conditions.

continue uses the last point of the previous integration as the new initial condition and continues to solve the equations.

Load

Instead of typing in a new set of parameters each time one runs the program, one may load the values from an option file by choosing the load option from the main menu. Pressing this button brings up the search path for a file. Complete the path name to the desired subdirectory and press the **return** key. A scrolling window appears which displays the content of a subdirectory. Use the arrow keys or scroll bar to move through the list of files; select a file by highlighting it and pressing the **Okay** button. Press **Cancel** to return to the main menu.

Initial conditions

The window for choosing for the initial conditions of the simulation is similar to that for setting the parameters. Each state variable is initialized by clicking the appropriate state button (x, y or z), and either incrementing/decrementing the current values by mean of the up and down arrows, or typing the value in the dialogue box and pressing **modify**. The default values are : $x_0 = y_0 = z_0 = 0.1$. Note that if one uses **continue** in the menu **Parameters** to integrate the equations, he can press **initial condition** in the main menu and henceforth obtain the coordinates of a current point on the trajectory (the initial condition of the next iteration).

Algorithm

In our program, the user may choose to solve Chua's dimensionless equations by means of the forwards Euler, fourth order Runge-Kutta, or sixth order Adams-Bashforth algorithm. The user specifies the value of the integration step. He also gives an upper bound on the relative local truncation error $|T_n|/|x(t_n)|$. The program puts out an alert if the current step size causes the LTE estimate to exceed the bound.

plOt

Choose what you want to display on the screen : eigenplanes and eigenvector in the **middle** region and in the **outer** regions , **boundary** planes, equilibrium **points**. When the button is lighted, the corresponding element is displayed. The users can also choose the **speed** option which displays the trajectory slowly so that he can have a better understanding of the evolution of the trajectory. This is particularly interesting when the eigen elements are displayed. When the selections are done, press **Okay** and the graphic display appears.

If you click on the button of the mouse with the cursor inside the graphic screen, a menu appears that allows one to rotate the attractor, either step by step (10 degrees) or automatically by chosing the option **auto**. To exit the menu type **cancel**. **reset** sets back the attractor to its initial position (before any rotation). For convenience, it is also possible to rotate the attractor directly from the keyboard without even selecting the rotation menu : Q and A rotate the attractor around the axis X in both directions, W and S around the axis Y, and E and D around the axis Z.

[28] except for Plot, type O

Save

The save option prompts the user for the names of files in which to save options and/or data from a simulation. Data files include the parameters for the simulation as a header and are written in ASCII format.

Quit

The **quit** button exits the program gracefully

8.2 Appendix B : eigenvalues, parameters and Lyapunov dimension for the gallery of attractors

In this last appendix we have collected the data relative to the gallery of attractors in table 1. For each attractor, we first give the number of the figure where it is displayed, the Lyapunov dimension, the eigenvalue pattern [29] and the parameters of the dimensionless equations.

[29] μ_1, μ_2 , and μ_3 are the eigenvalues corresponding to the inner region. As mentioned in section 2.1 in the outer region we always find one real real and two complex-conjugate eigenvalues, and therefore it is possible to divide the system by a non-zero positive number and assume that the imaginary part of the complex eigenvalues has a norm equal to one. With the notations used in the table : $\nu_1 = \gamma_1, \mu_2 = \sigma_2 + j1.00$ and ,$\mu_3 = \sigma_2 - j1.00$

Table 1 : a gallery of attractors

Fig	dim	Eigenvalues					Canonical parameters					
		μ_1	μ_2	μ_3	γ_1	σ_2	α	β	γ	a	b	k
6	2.14	0.667	-0.304	±j 0.901	-1.22	-0.304	8.5	14.28	0.0	-1.142	-0.7142	1
7	2.11	0.728	-0.317	±j 0.889	-1.29	0.061	9.0	14.28	0.0	-1.142	-0.7142	1
11	2.09	1.15	-2.98	-5.70	-0.892	0.150	-4.925	-3.649	0.0	-2.497	-0.9301	1
19a	2	0.634	-0.0479	±j 1.013	-.419	0.0275	1800	10000	0.0	-1.026	-0.982	1
19b	2.09	0.2574	-0.7129	±j 1.145	-0.7792	0.45159	-4.087	-2.00	0.0	-1.1429	-0.7142	1
19c	2.185	0.1144	.5657	±j 1.211	-0.3496	0.4119	-6.691	-1.520	0.0	-1.1429	-0.7142	1
19d	e13	-1.615	0.08336	±j 1.149	0.9212	-0.4122	8.342	11.925	0.0	-0.7048	-1.146	1
19e	2.03	0.7545	-0.2430	±j 0.9059	-1.322	.0651	15.6	28.58	0.0	-1.143	-0.7142	1
19f	2.007	0.7545	-0.2430	±j 0.9059	-1.322	.0651	15.6	28.58	0.0	-1.143	-0.7142	1
12	2.0	0.2055	-0.04794	±j 1.004	-0.1381	-0.03419	31.53	64.25	-0.6683	-0.9926	-1.023	-1
15	2.07	1.418	-0.0161	±j 1.006	-0.997	0.01695	13.32	2 13.1	-0.9408	0.474	-2.039	-1
16	2.03	-0.799	0.009276	±j 0.406	0.9223	-0.8673	-90.36	-89.11	-1.000	-0.9889	-0.9884	-1
17	2.1	0.50	-0.5764	±j 0.9135	-1.122	0.2005	52.056	54.29	-1.000	-1.0181	-1.0200	-1
18	2.04	-0.6316	0.00635	±j 0.3802	0.9395	-0.8005	-100.18	-98.82	-1.00	-.99002	-.9893	-1
20a	2.30	0.272	-0.136	±j 0.409	-0.409	0.0454	-1.424	0.02944	0.3226	-0.0715	-0.1817	1
20b	2.06	0.618	-0.37	±j 3.5	-2.30	0.195	-1.559	0.01564	0.1574	-0.2438	-0.04251	-1
20c	2.27	0.20	0.30	±j 10.0	-3.00	0.30	-1.083	0.0000969	0.007327	-0.09411	0.0001899	-1
20d	2.39	0.30	0.0577	±j 2.78	-1.33	0.29	-1.233	0.007233	0.08758	-0.1767	-0.01626	-1
20e	2.24	0.44	0.0577	±j 2.78	-1.33	0.29	-1.318	0.01257	0.1328	-0.2241	-0.02811	-1
20f	2.27	1.474	-0.487	±j 1.0	-1.04	0.0343	3.7091	24.07	-0.8592	-2.764	0.1805	1
20g	2.032	0.527	0.0948	±j 2.011	-20.61	0.1384	-75.0	31.25	-3.125	-0.98	-2.4	1
20h	2.014	-10.248	0.0688	±j 0.4971	0.2619	0.04714	-75.0	31.25	-3.125	-2.4	-0.98	1
20i	2.17	-0.07620	-0.06497	±j 0.74	-0.0762	0.005615	-1.609	0.0704	0.2973	-0.1392	-0.2175	1
20j	2.17	1.032	0.1354	-0.4425	0.020	-.20	-17.38	1.413	1.045	-1.525	-0.4576	-1
20k	2.19	0.919	-0.541	-3.64	-3.53	0.156	-1.461	-0.09422	-0.3230	1.219	-0.5141	-1
20l	2.13	6.80	4.30	2.50	-9.0	0.01	-1.301	-0.0136	-0.02969	0.1690	-0.4767	1

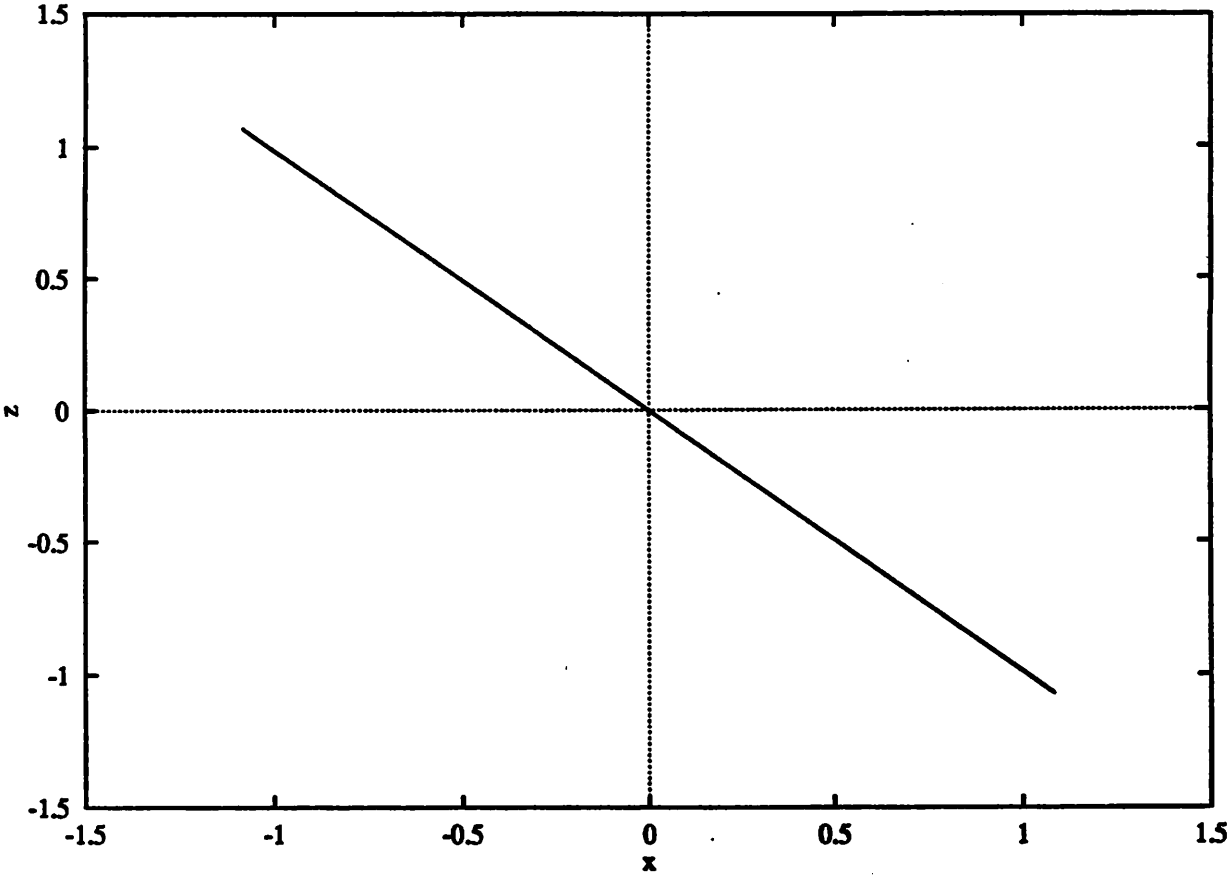

Fig. 16c

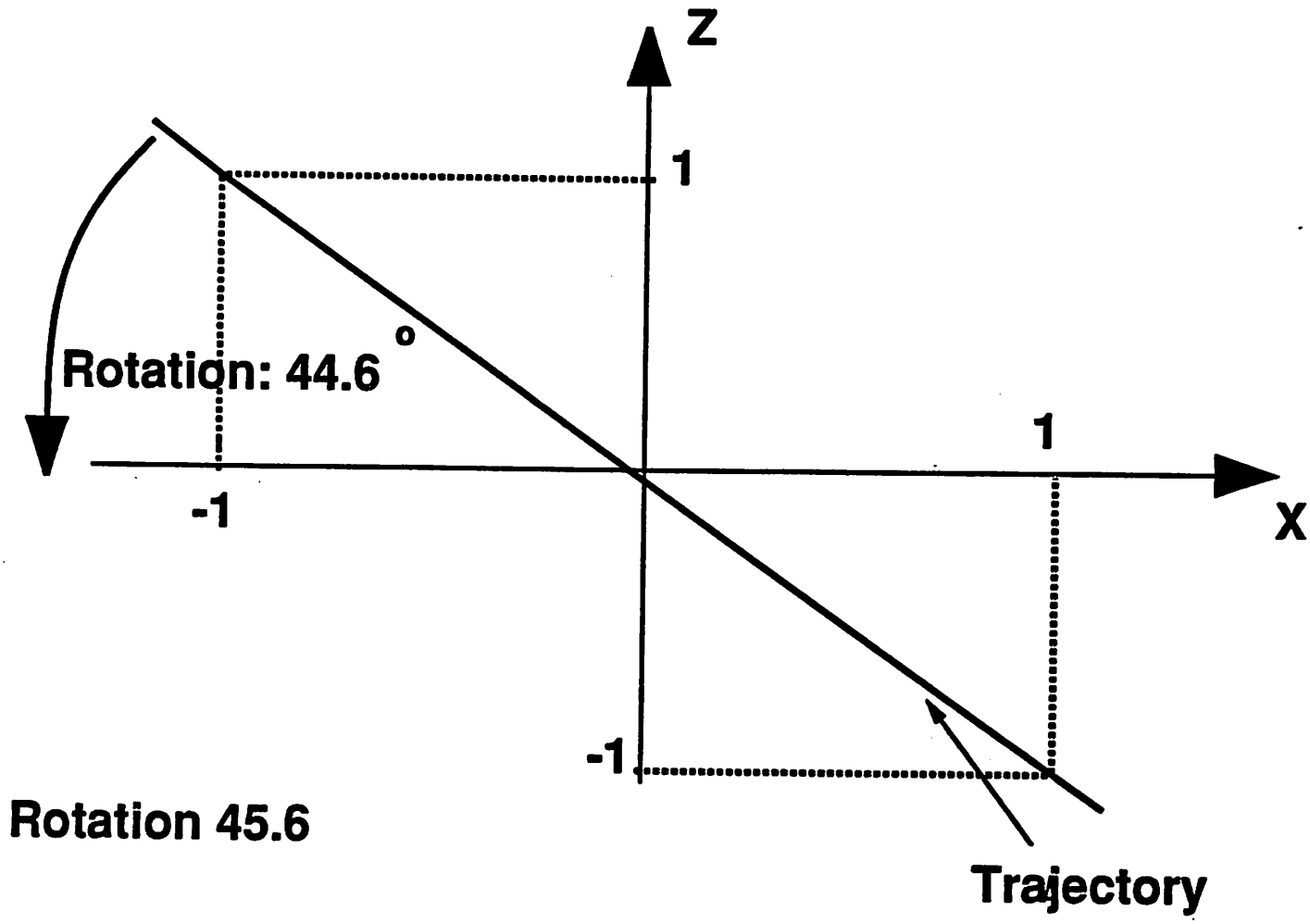

Fig. 16d

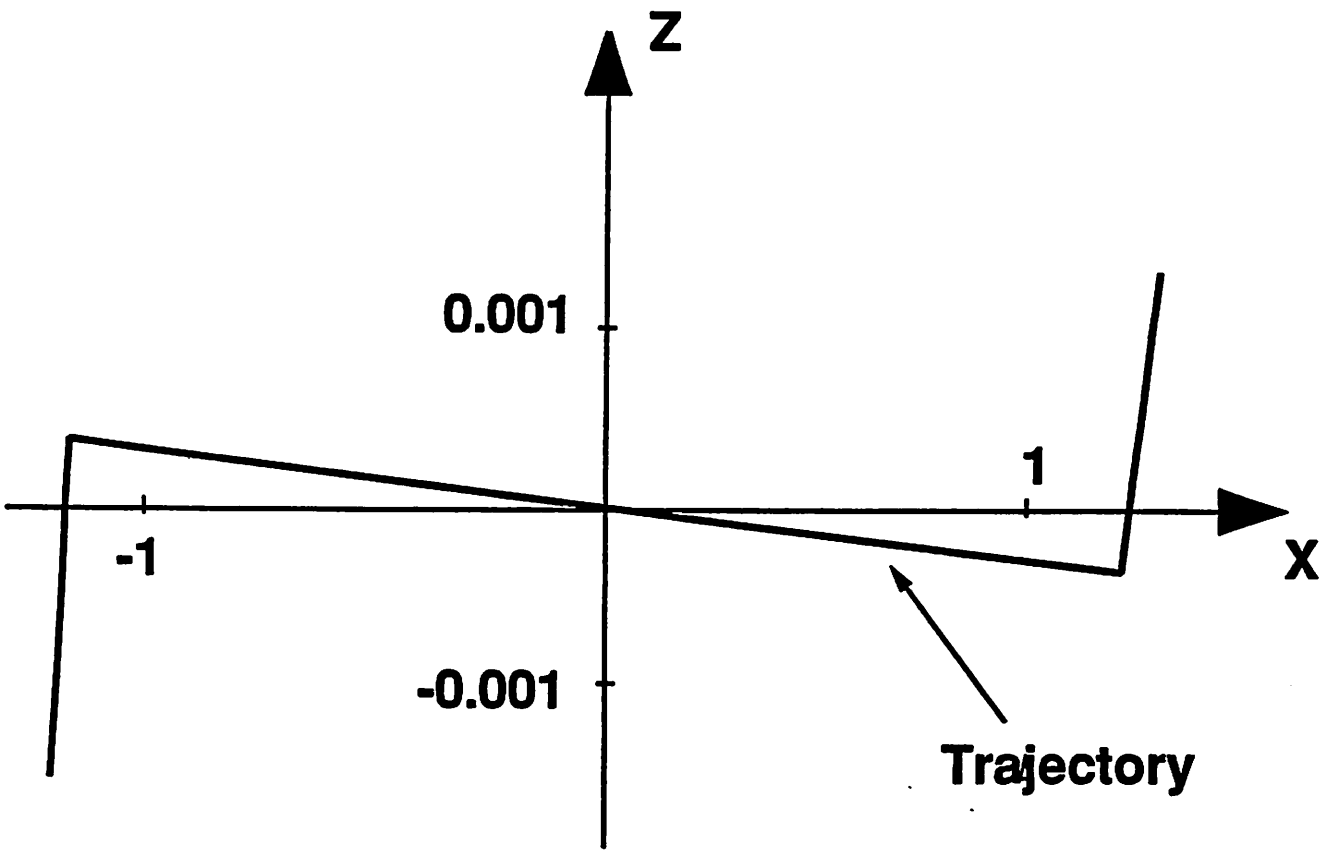

Fig. 16e

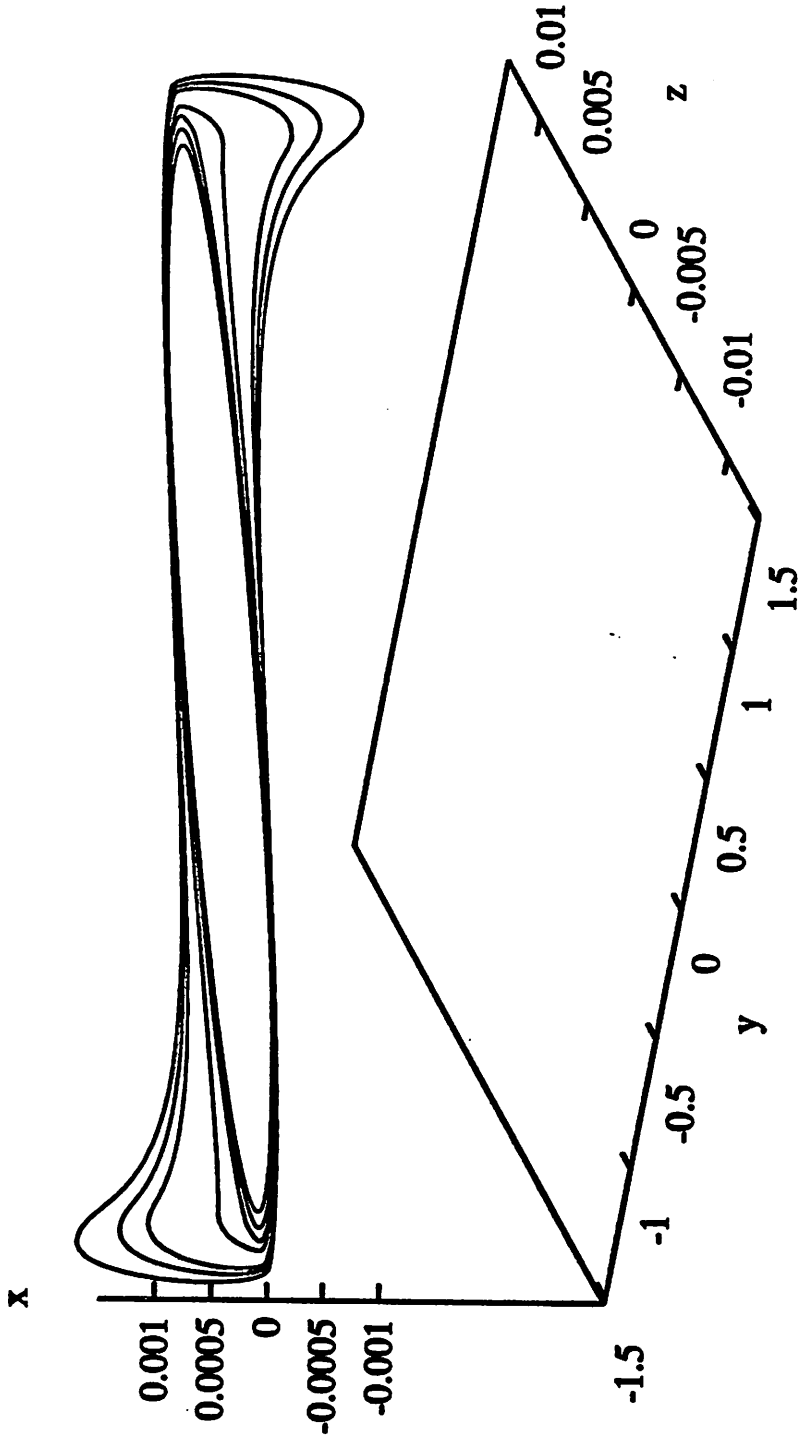

Fig. 16f

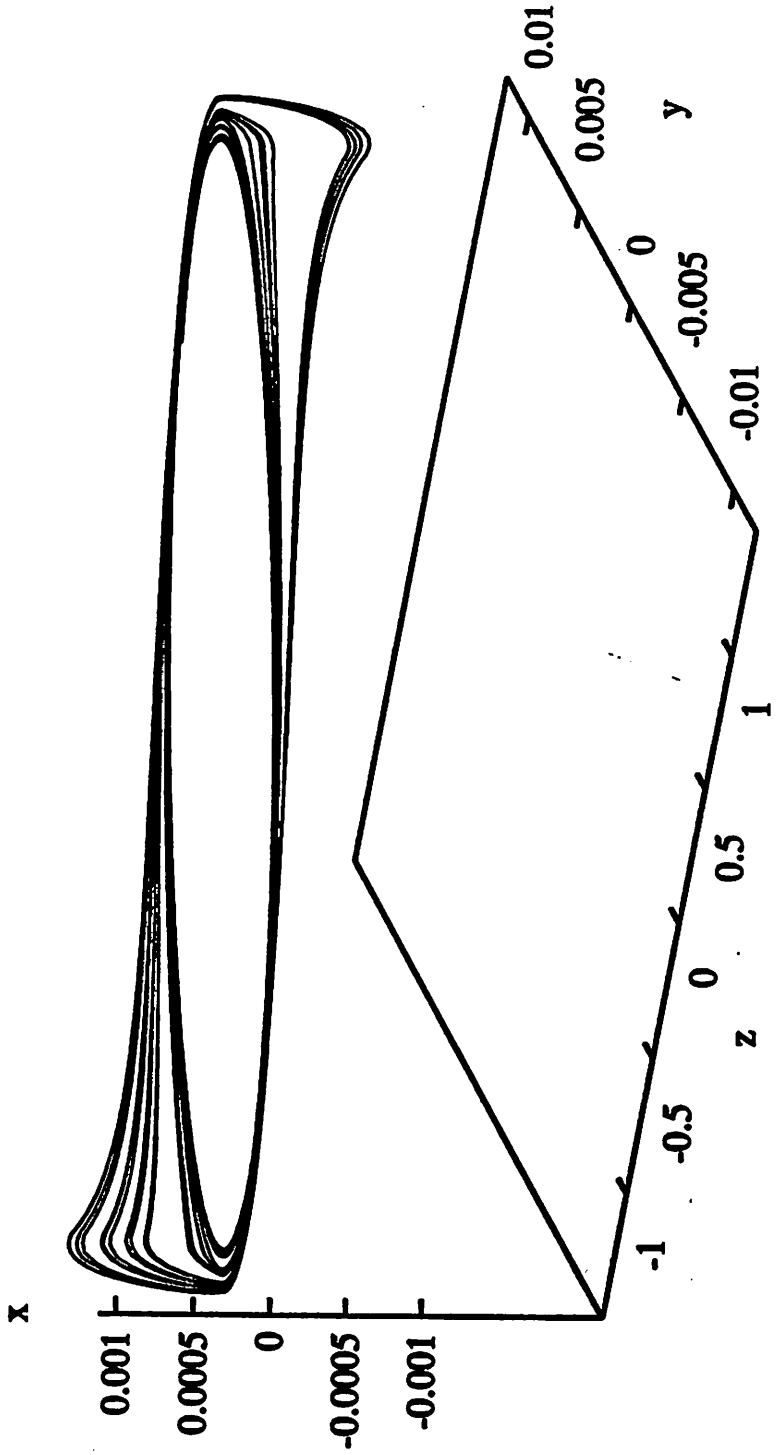

Fig. 18c

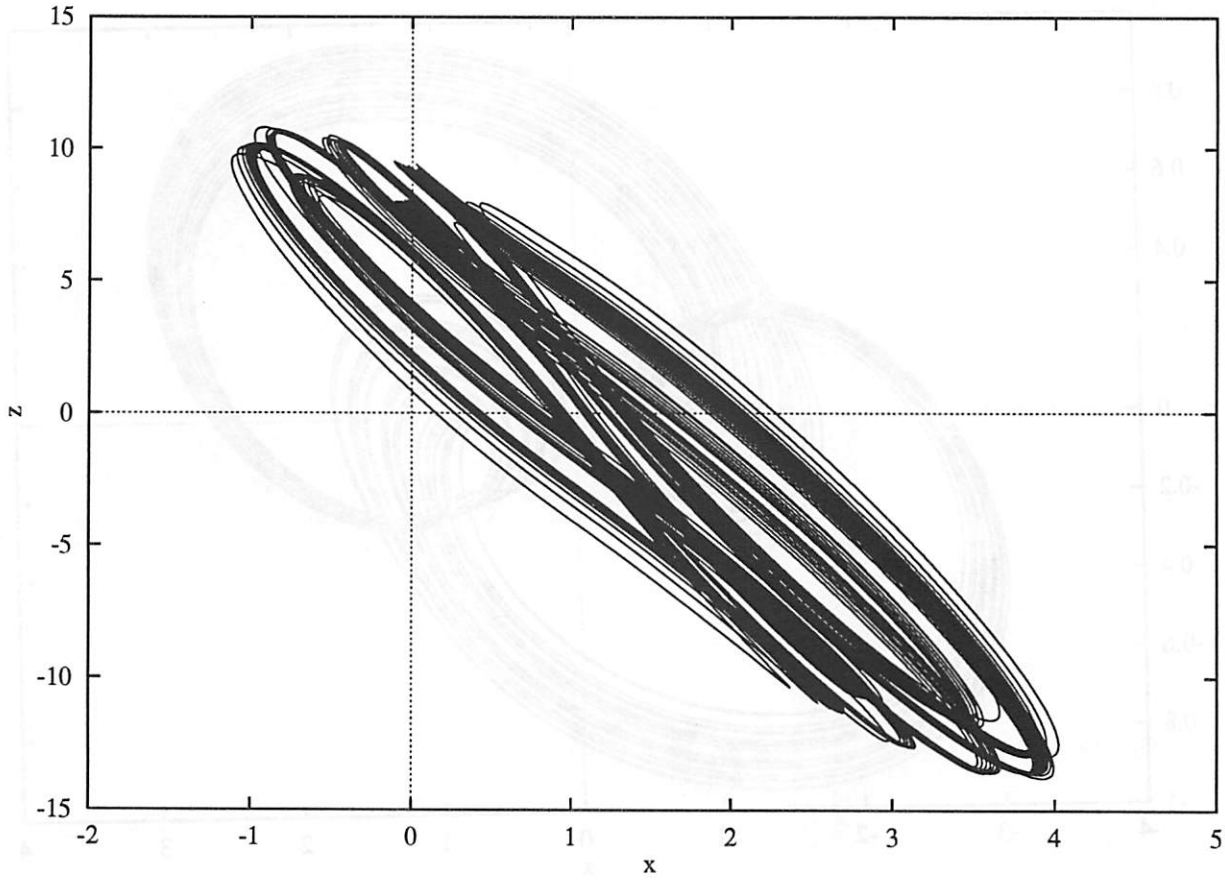

Fig. 19a

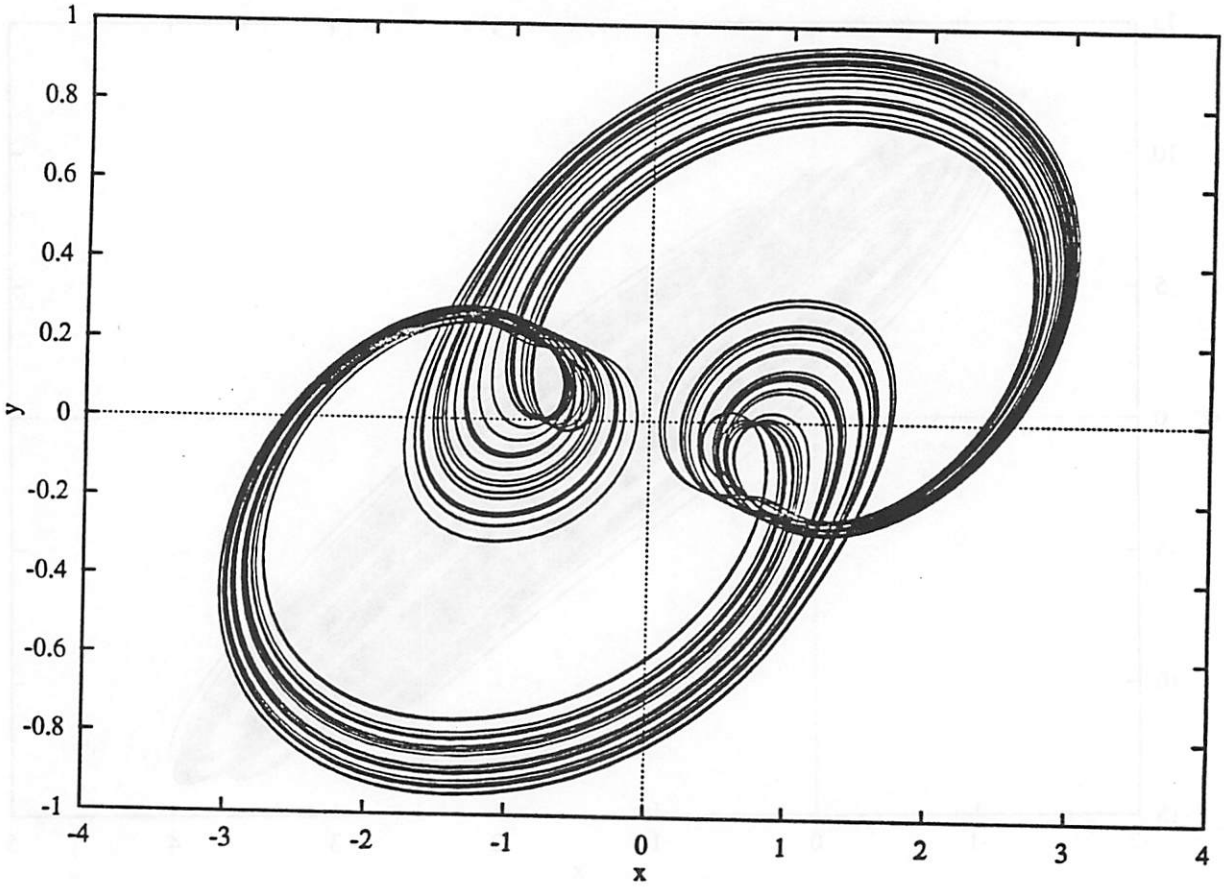

Fig. 19b

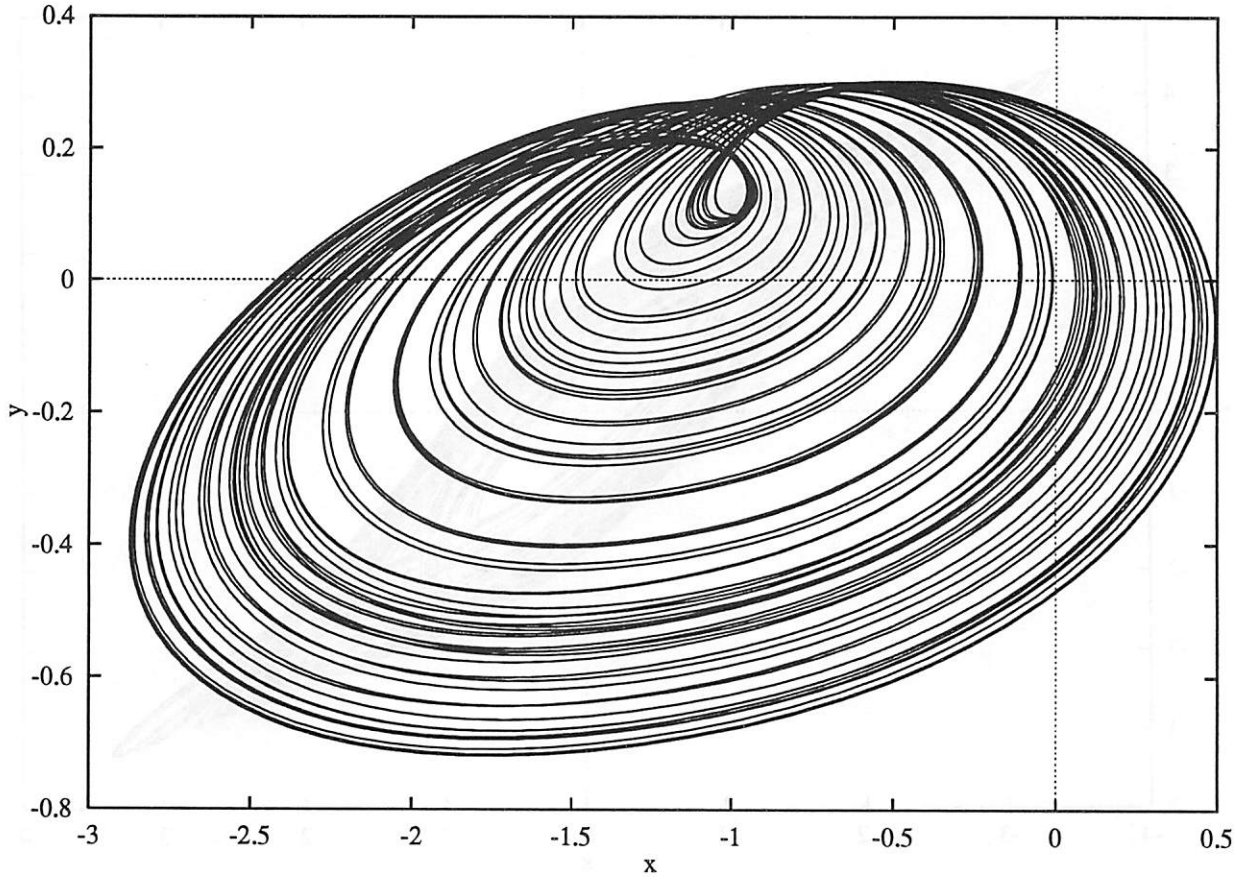

Fig. 19c

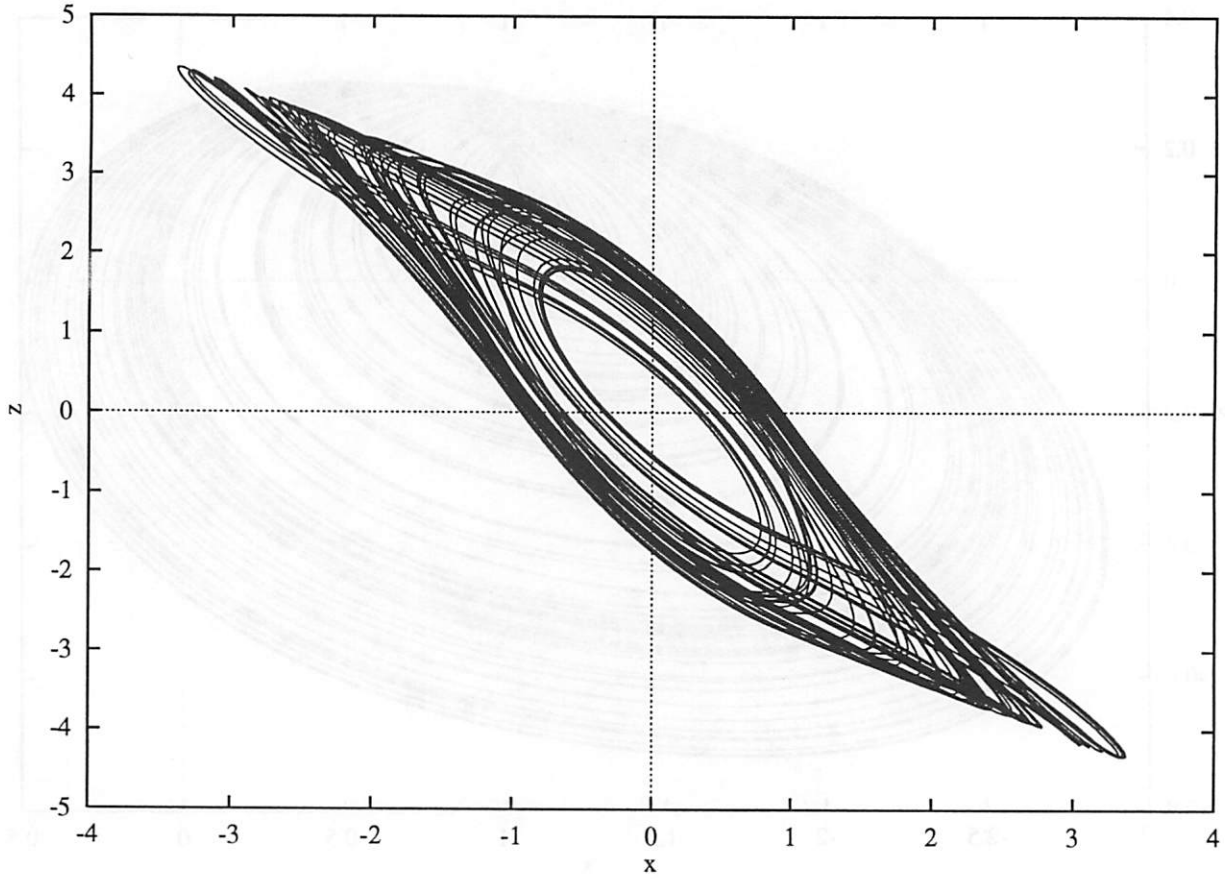

Fig. 19d

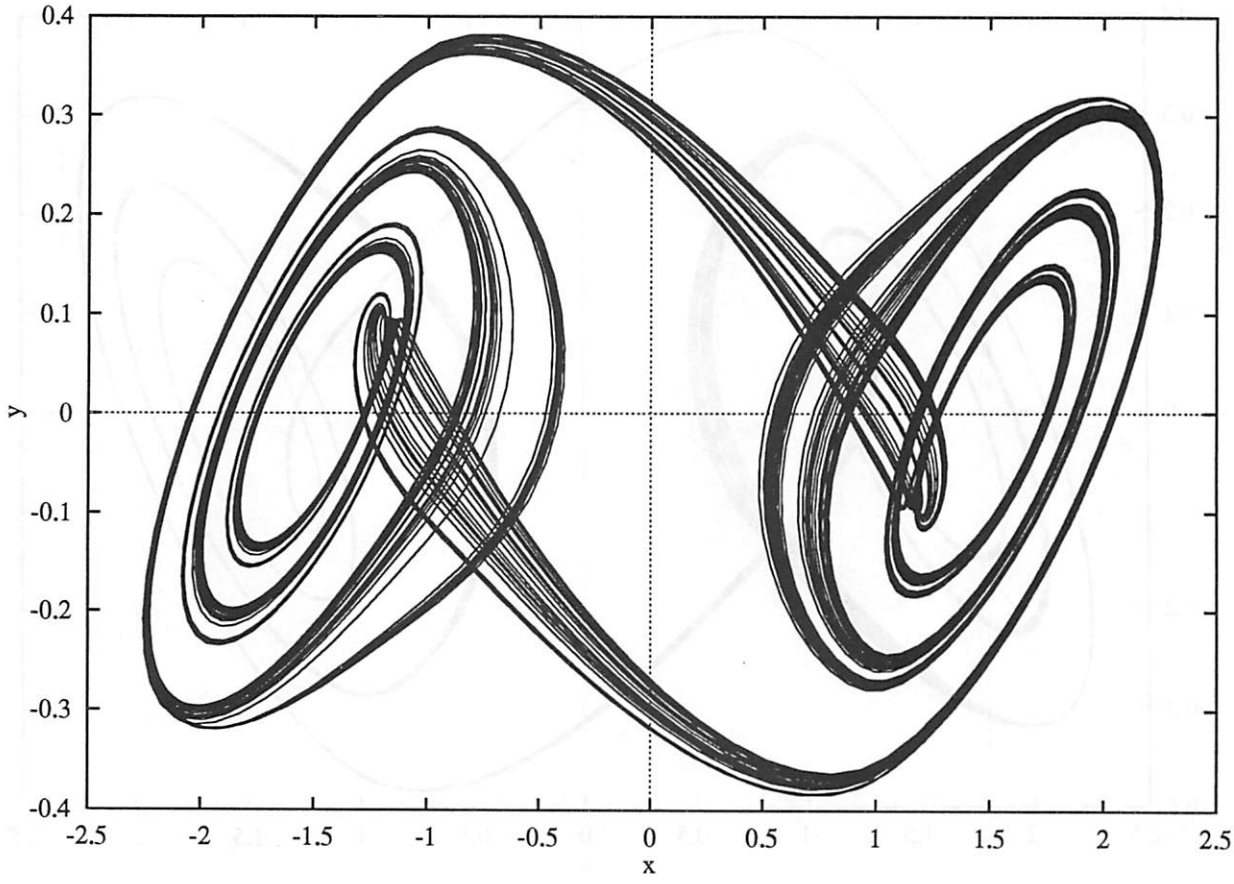

Fig. 19e

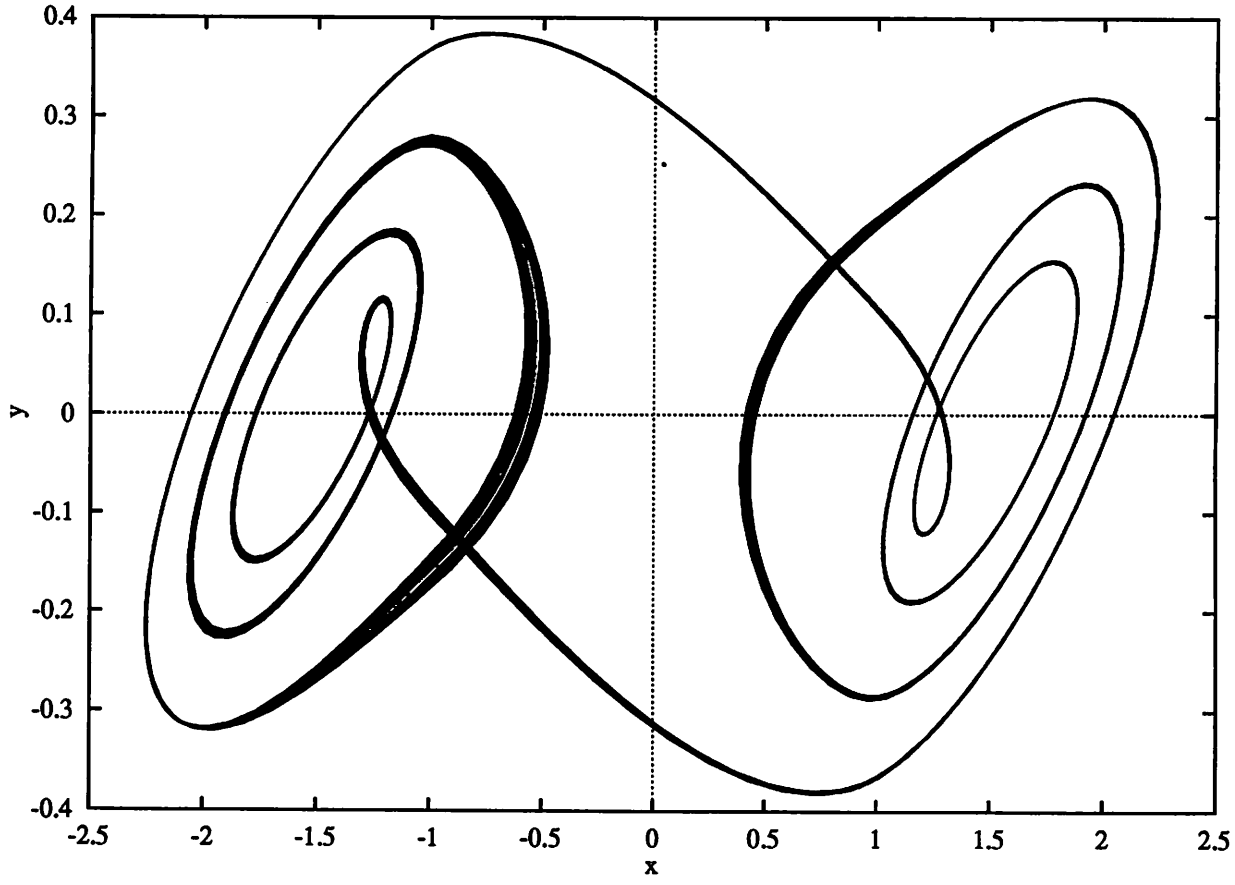

Fig. 19f

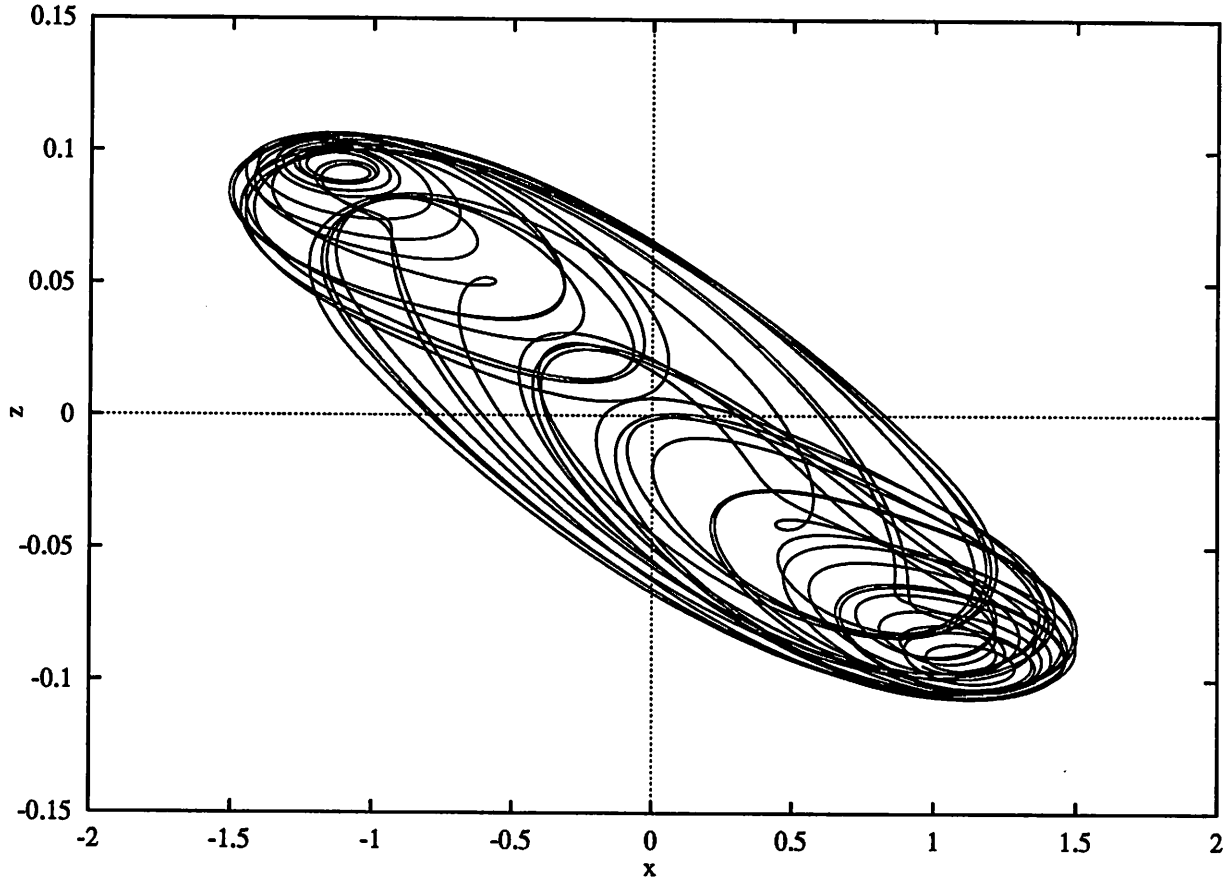

Fig. 20a

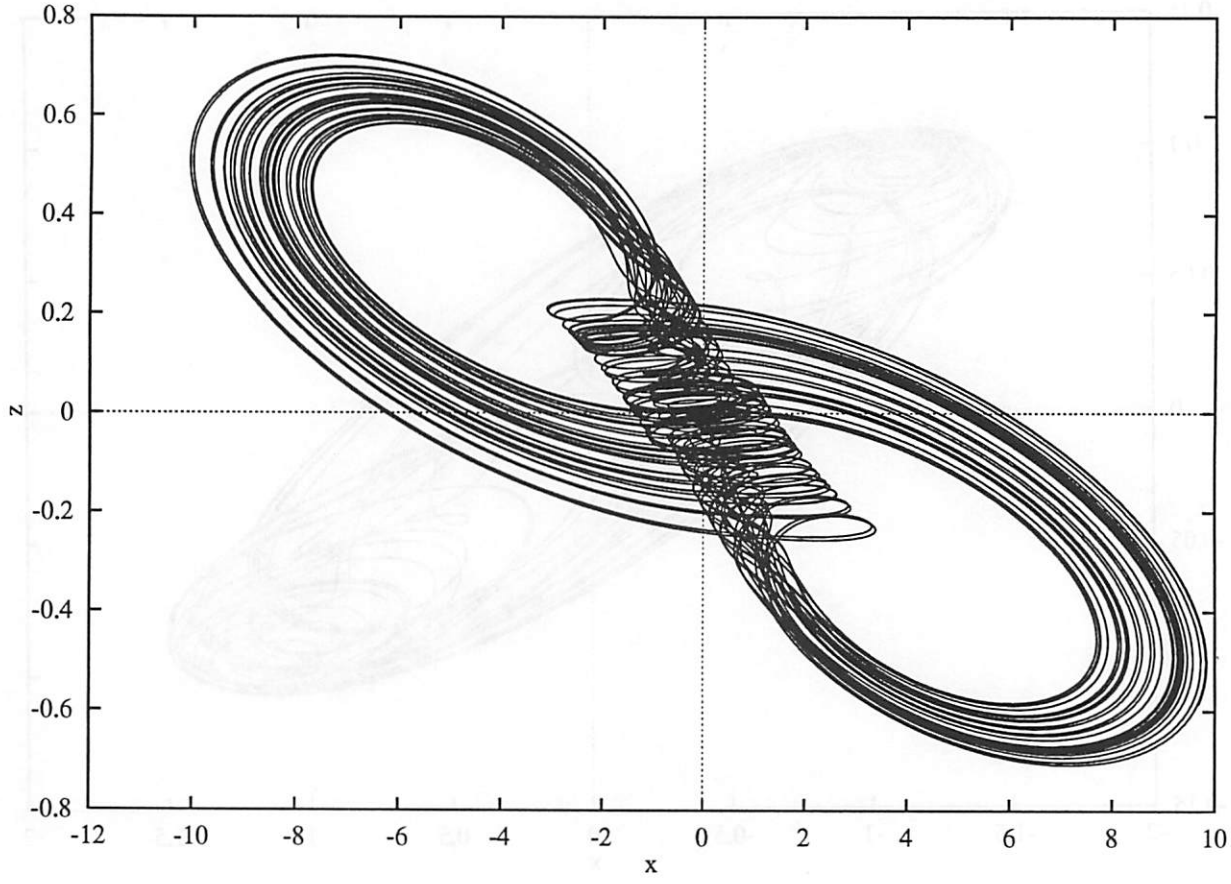

Fig. 20b

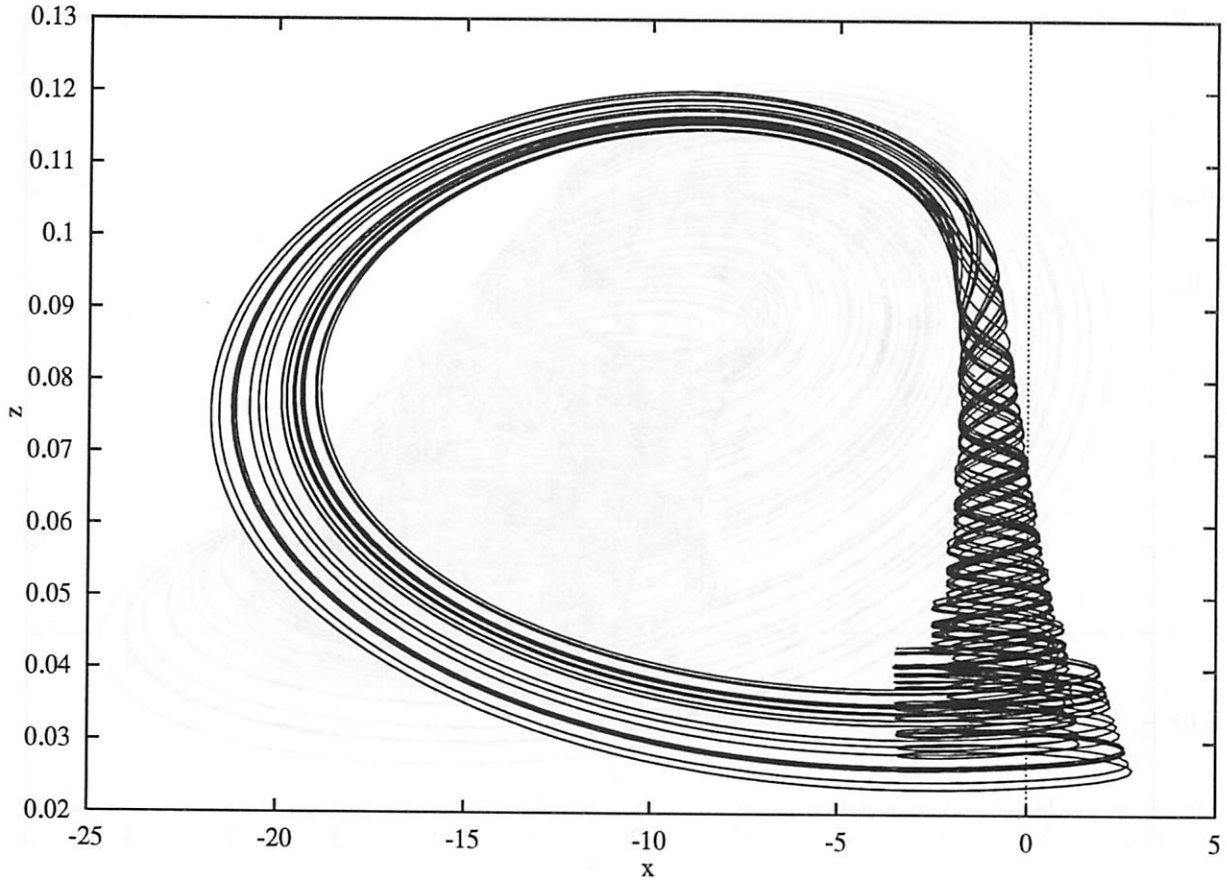

Fig. 20c

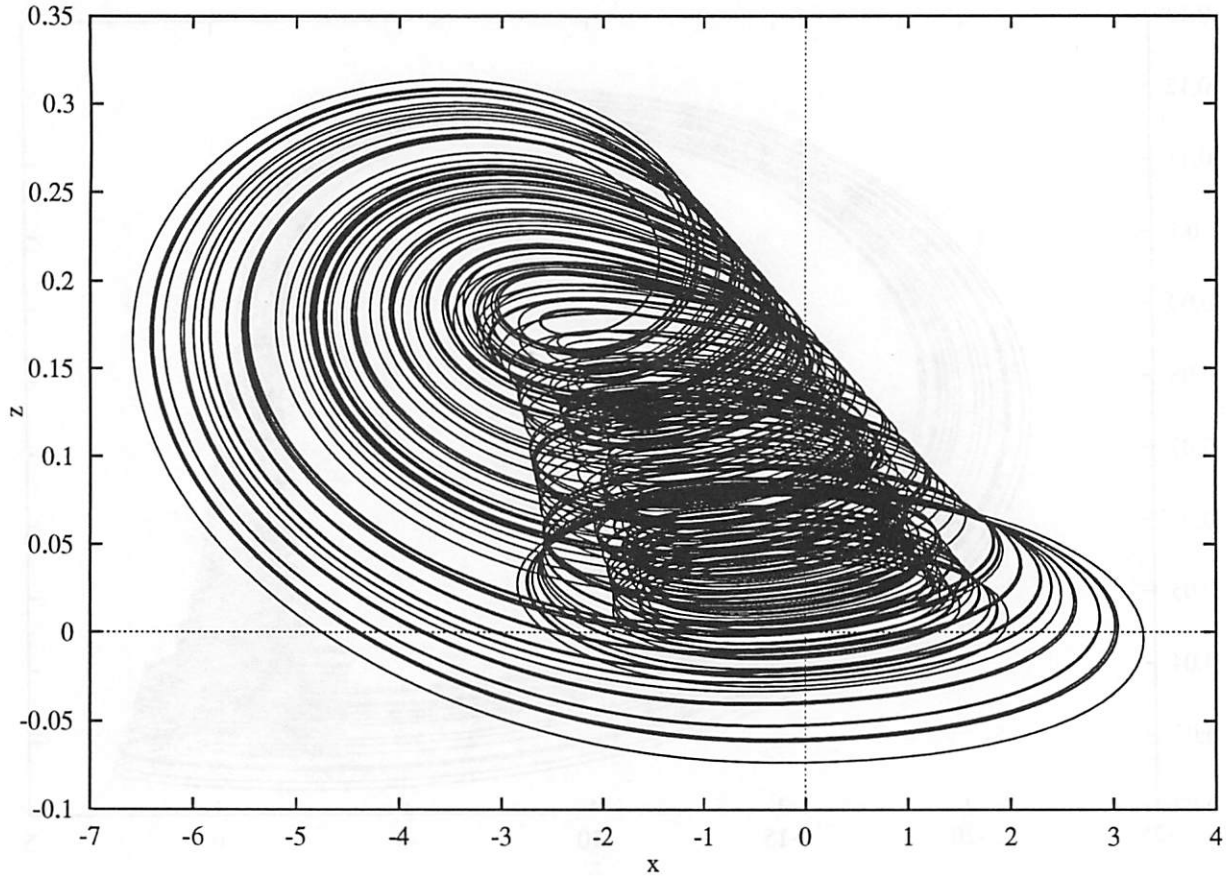

Fig. 20d

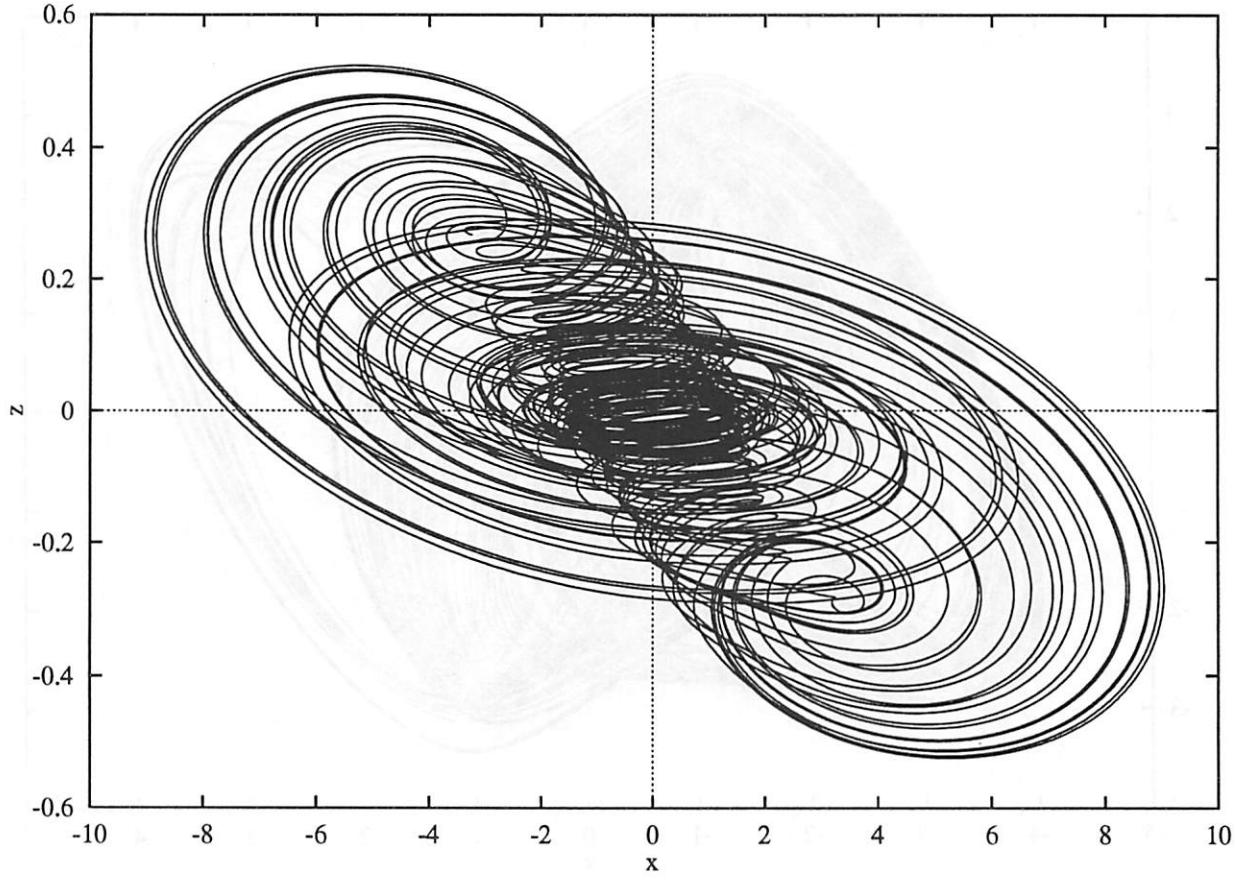

Fig. 20e

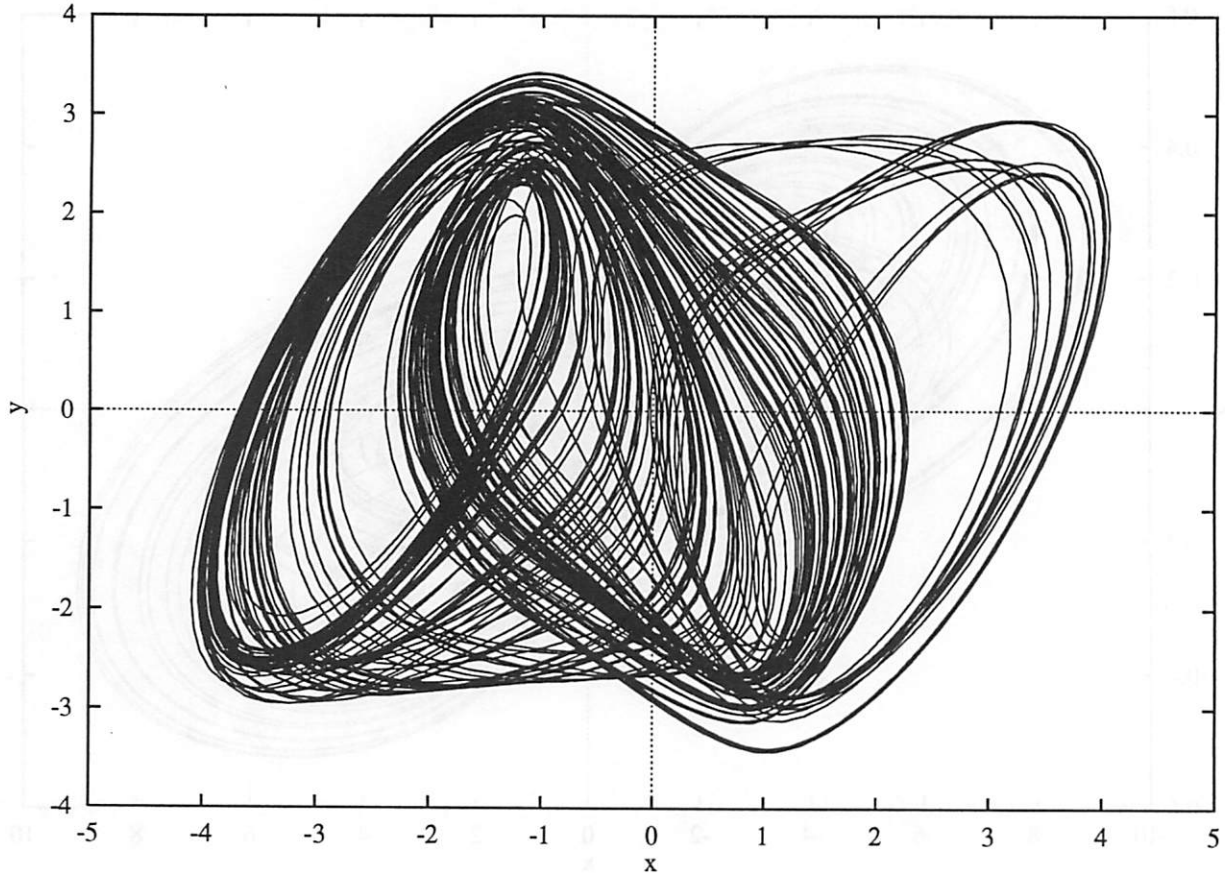

Fig. 20f

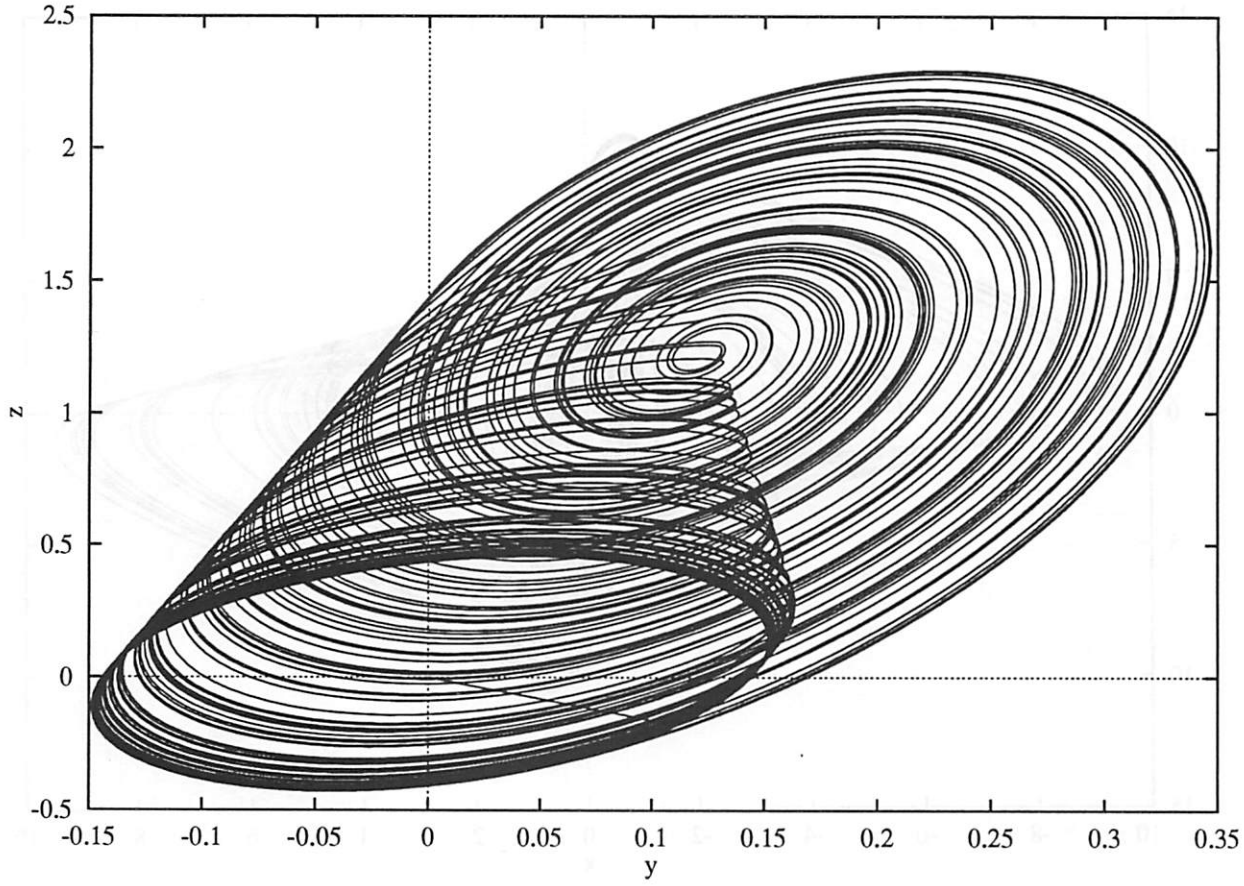

Fig. 20g

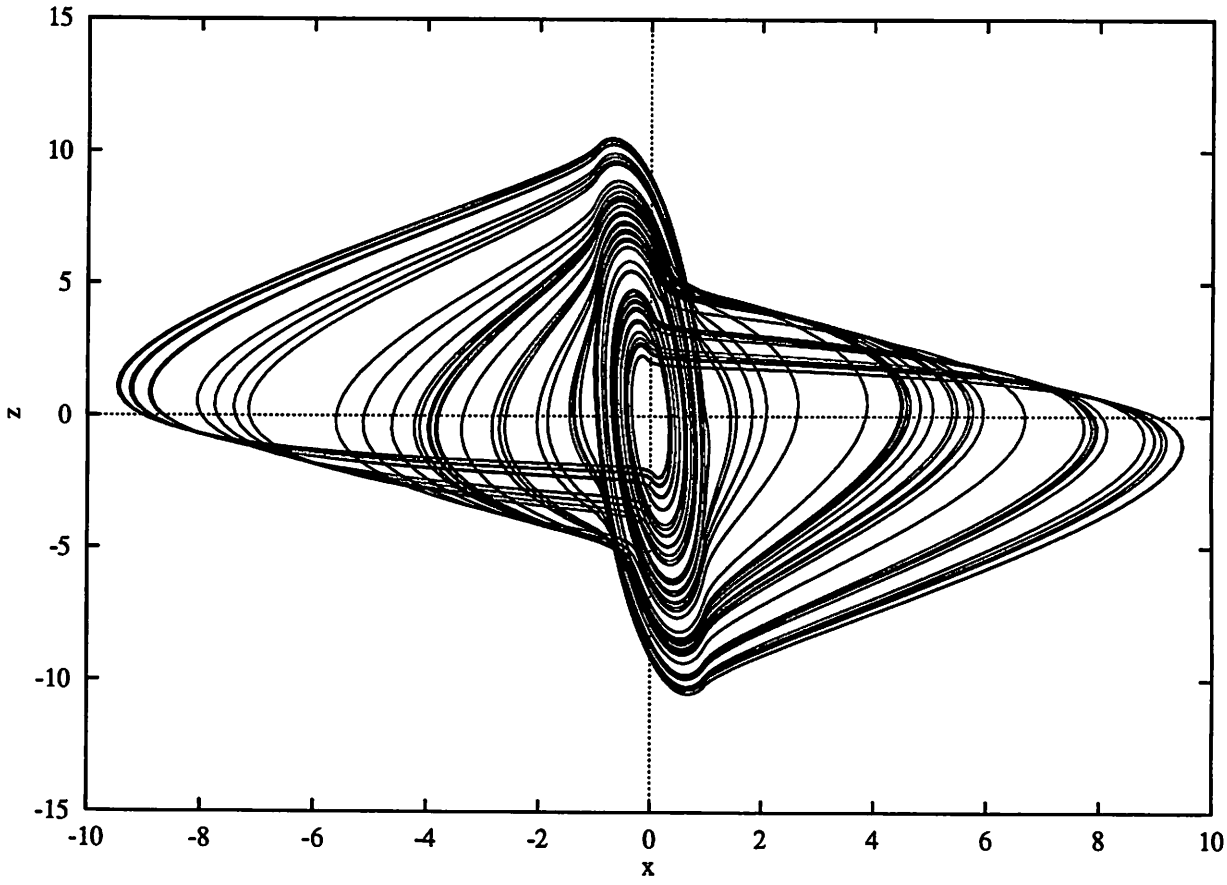

Fig. 20h

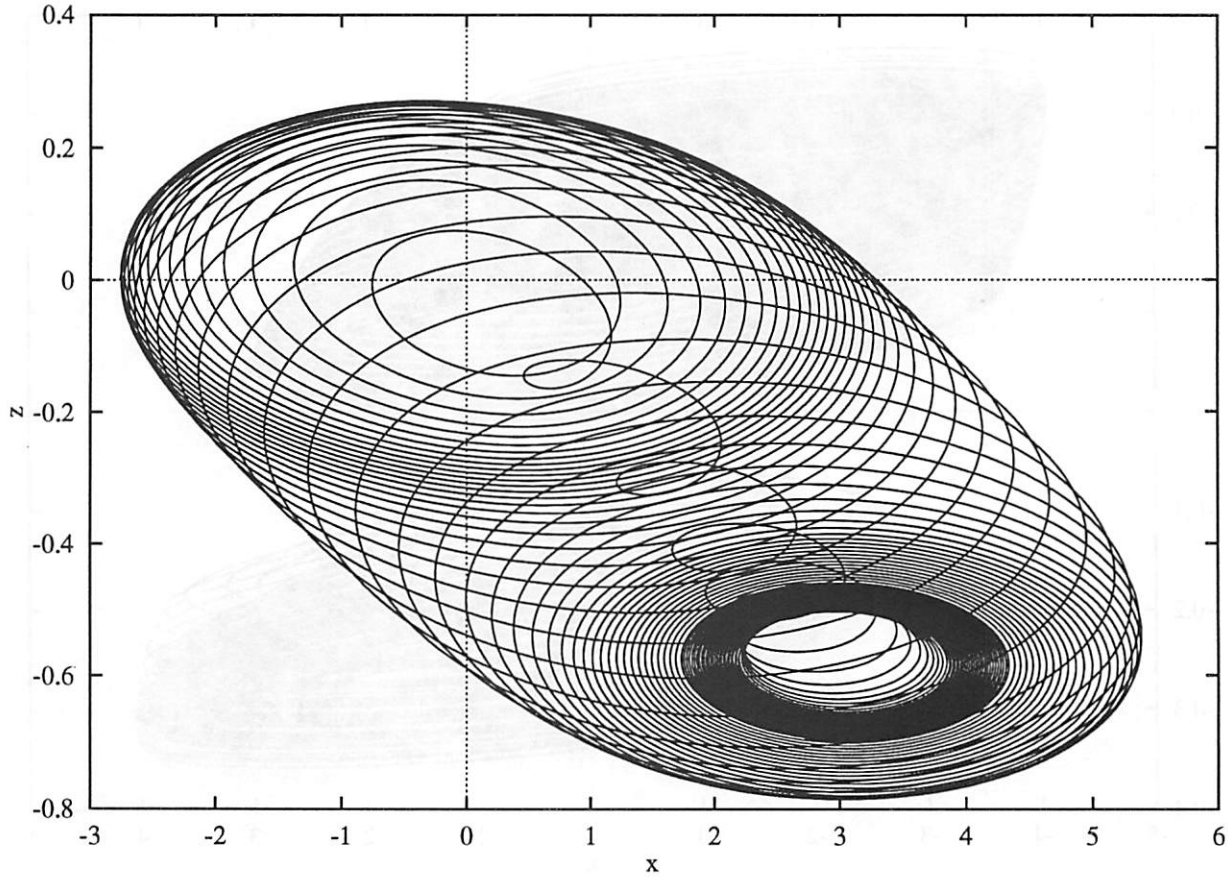

Fig. 20i

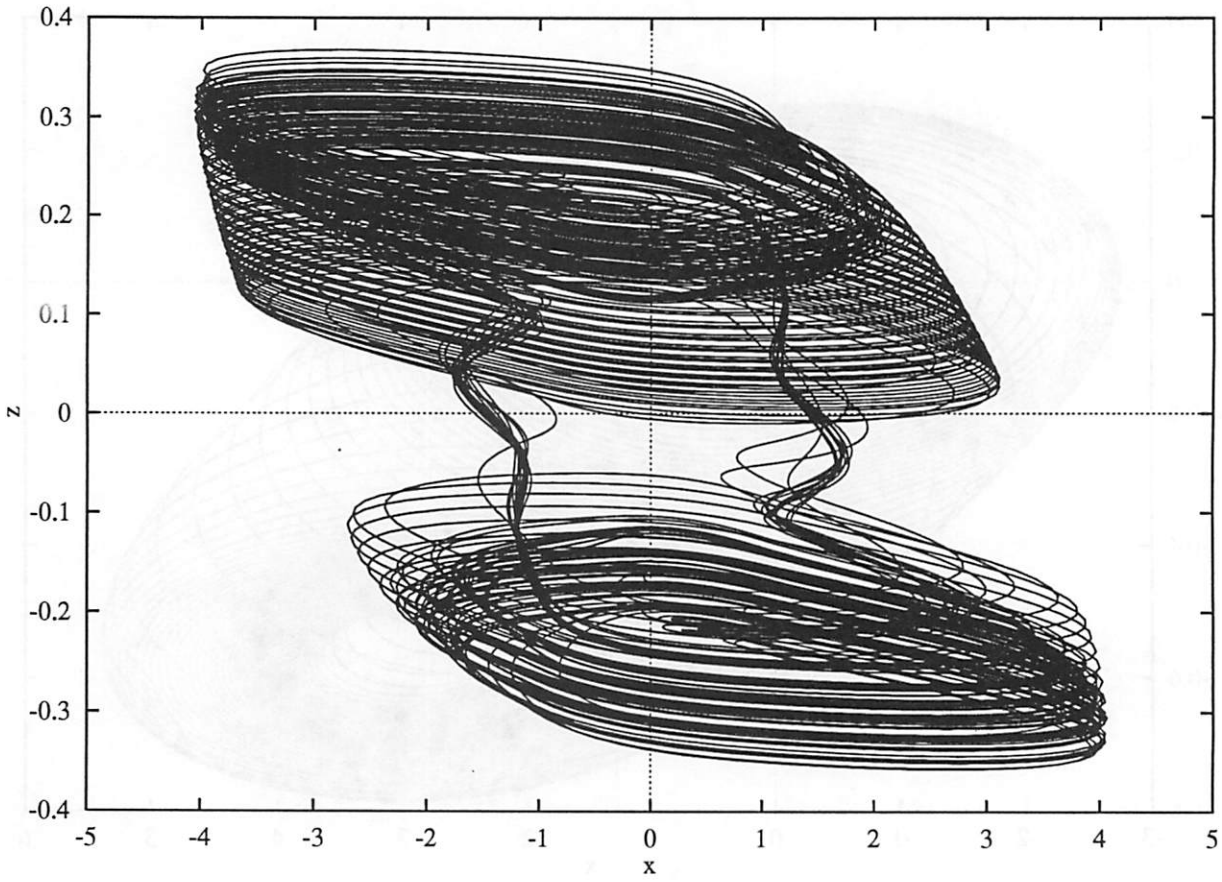

Fig. 20j

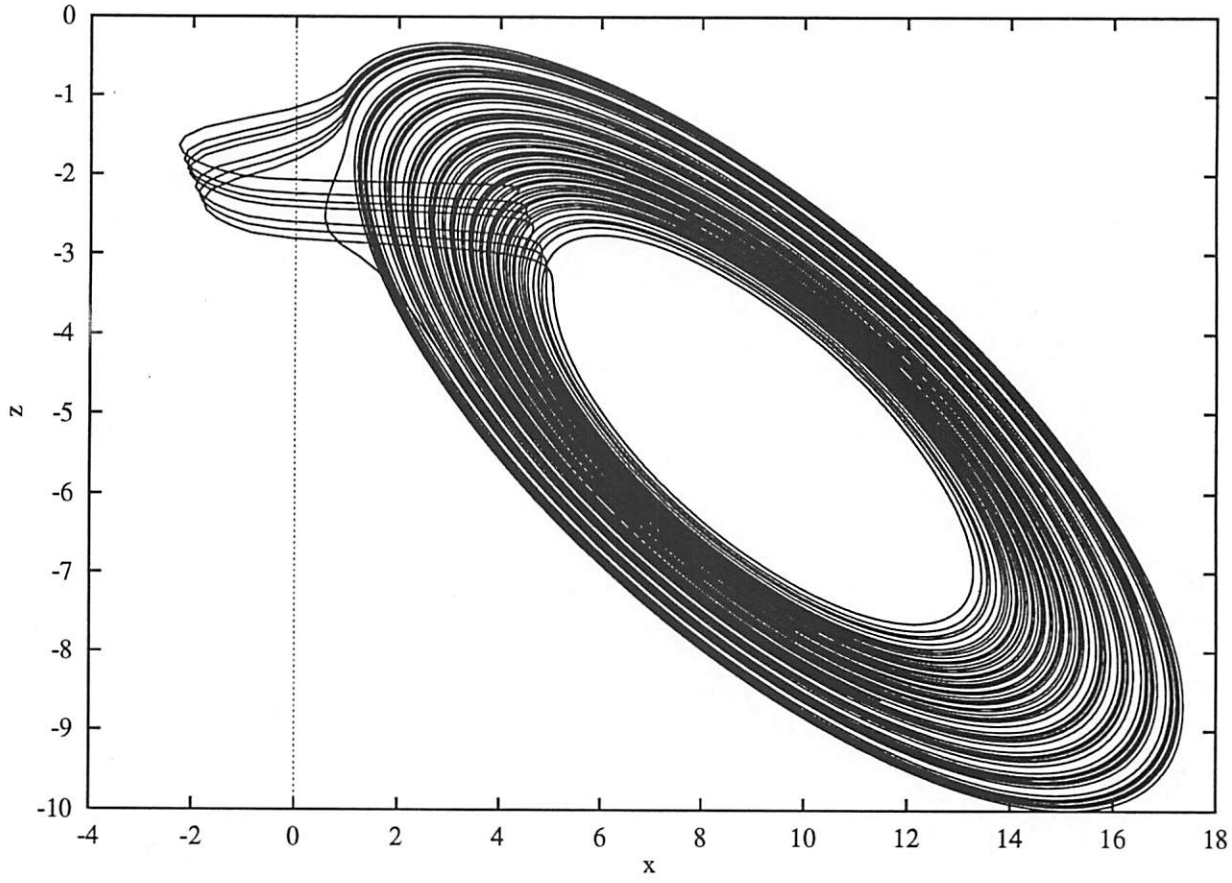

Fig. 201